

ATTACHMENT A-1

**THE ESTIMATION OF EXTERNAL DOSES FROM
DEPOSITED RADIONUCLIDES FOLLOWING THE
ACCIDENT AT THE FUKUSHIMA DAIICHI NUCLEAR
POWER STATION AND THEIR VALIDATION**

UNSCEAR 2020/2021 Report, annex B, Levels and effects of radiation exposure due to the accident at the Fukushima Daiichi Nuclear Power Station: implications of information published since the UNSCEAR 2013 Report

Content

This attachment describes the model used to estimate external doses from deposited radionuclides in the Committee's update of the doses estimated in the UNSCEAR 2013 Report. The model is based on that used in the UNSCEAR 2013 Report but has been improved to take account of extensive monitoring data collected in the years following the accident from car-borne surveys and those carried out on foot. Comparisons have been made with the results of numerous personal dosimetry campaigns, carried out at various times and locations within Fukushima Prefecture, and the model has been validated for wider use within areas of Japan affected by the accident at the Fukushima Daiichi Nuclear Power Station (FDNPS).

Notes

The designations employed and the presentation of material in this publication do not imply the expression of any opinion whatsoever on the part of the Secretariat of the United Nations concerning the legal status of any country, territory, city or area, or of its authorities, or concerning the delimitation of its frontiers or boundaries.

Information on Uniform Resource Locators (URLs) and links to Internet sites contained in the present publication are provided for the convenience of the reader and are correct at the time of issue. The United Nations takes no responsibility for the continued accuracy of that information or for the content of any external website.

© United Nations, February 2023 (corrected).¹ All rights reserved, worldwide.

This attachment has not been formally edited.

¹ Tables A-1.13, A-1.15 and the title of table A-1.16.

CONTENTS

I. EXTERNAL DOSE ASSESSMENT IN THE UNSCEAR 2013 REPORT	5
II. RADIATION MONITORING OF AMBIENT DOSE RATES IN JAPAN SINCE THE ACCIDENT	6
III. REVISION OF THE DOSE ASSESSMENT METHODOLOGY FOR M2020	7
A. Motivation	7
B. The computational schema	7
C. Radionuclide composition of the deposited radioactive material	7
D. Dose rate coefficients for external exposure from radioactive material deposited on the ground	11
E. Dynamics of ambient dose rates due to downward migration and weathering	13
F. Dynamics of ambient dose rates in populated areas	15
G. Shielding factors for houses	17
H. Fractions of time spent in various locations (occupancy factors)	17
I. Summary of M2020	19
IV. VALIDATION OF M2020 FOR DOSES FROM EXTERNAL EXPOSURE	20
A. Scenario A: The Fukushima Health Management Survey	20
B. Personal dosimetry studies	22
C. Outcomes of the personal dosimetry surveys in Minamisoma City and Naraha Town for 2014–2019	28
D. Summary	35
E. Variability of individual external doses in Fukushima Prefecture	36
V. RESULTS OF THE MODEL CALCULATIONS	37
A. Cumulative doses of external exposure per unit ¹³⁷ Cs deposition density	37
B. Doses from external exposure in the first year following the Fukushima Daiichi Nuclear Power Station accident	39
C. Cumulative doses from external exposure for the population of Japan	40
D. Post-remediation doses	41
VI. SUMMARY	44
REFERENCES	47

I. EXTERNAL DOSE ASSESSMENT IN THE UNSCEAR 2013 REPORT

1. The external dose assessment methodology applied in the UNSCEAR 2013 Report [UNSCEAR, 2014] was largely based on post-Chernobyl experience gathered in territories of the Republic of Belarus, the Russian Federation and Ukraine contaminated by radioactive material [Golikov et al., 2002; Jacob, 1996; Likhtarev et al., 2002]. The model applied in the UNSCEAR 2013 Report had used pragmatic approximations and parameters and is briefly summarized below.

2. The effective dose rate $\dot{E}_i(t)$ for a person from age/social group i at time t after the deposition of radionuclides was calculated as follows:

$$\dot{E}_i(t) = r(t)A_{\text{Cs-137}} \sum_m \frac{A_m}{A_{\text{Cs-137}}} e^{-\lambda_m t} \dot{d}_{m,i}^{\text{eff}} \sum_j f_j(t) p_{ij} \quad (\text{A-1.1})$$

where A_m is the initial deposition density of the radionuclide m at 15 March 2011 (Bq/m^2); λ_m is its radioactive decay rate (s^{-1}); $\dot{d}_{m,i}^{\text{eff}}$ is the effective dose rate coefficient for the i^{th} age group attributed to the initial source configuration immediately after deposition of the radionuclide m ($\text{Sv}/\text{s}/(\text{Bq}/\text{m}^2)$); $r(t)$ is a phenomenological function representing the reduction with time of the dose rate in air above undisturbed soil due to migration of the radionuclide into the soil depth, weathering and runoff (unitless); $f_j(t)$ is the time-dependent location factor, i.e., a ratio of the ambient dose rate in air in a specific location to that above open ground undisturbed from the moment of deposition (unitless); $p_{ij}(t)$ is the fraction of time spent in various locations, termed here as occupancy factors, representing behaviour of an individual belonging to the age/social group i of the population of interest (unitless).

3. In the UNSCEAR 2013 Report [UNSCEAR, 2014], the dose rate coefficients used in the model for calculation of external exposures, hereafter termed as M2013, were essentially based on the effective dose per air kerma ratios for idealized irradiation geometries from the International Commission on Radiological Protection (ICRP) Publication 74 [ICRP, 1996] and the dose rate coefficients for the environmental sources in soil [Jacob et al., 1986; Petoussi-Henss et al., 2012; Saito and Petoussi-Henss, 2014]. Correspondingly, the effective dose rate coefficients were taken as constant within each of the three considered age groups: children of age 1, 10 years and adults. For organ doses, only absorbed dose to the thyroid was inferred from the voxel phantom data [Petoussi-Henss et al., 2012] for the same three age groups.

4. Location factors, used in M2013, represented the effects of external dose reduction in various anthropogenic or semi-natural environments: paved and unpaved surfaces, various types of houses or dwellings, etc. The location factors in M2013 were largely based on the post-Chernobyl experience and the values of their parameters were determined for conditions specific to areas in the Russian Federation and Ukraine contaminated by radioactive material. The distinctive features of the location factors in M2013 are their dependence on time and a significant reduction of dose within populated areas in comparison to those undisturbed.

5. The UNSCEAR 2013 Report [UNSCEAR, 2014] focused on providing dose estimates for the three representative age groups: 1-year-old infants representing babies and preschool children, 10-year-old children representing school children and 20-year-old person as an adult. Based on the housing conditions, the population was assumed to inhabit wooden, wooden fireproof and concrete houses and buildings. Daily activities outside homes (e.g., nursing, study

or occupation) were assumed to take place indoors in concrete buildings for preschool and school children and for indoor (office) workers.

6. Fractions of time assumed to be spent by different population groups in various locations were termed occupancy factors in M2013 and these were established based on the information provided by the Japanese authorities and national statistics [MIC, 2011].

7. The cumulative effective doses for members of the public were calculated by integrating the effective dose rate (equation A-1.1), taking into account age-dependent changes of the dose rate coefficients and the occupancy factors. The integral absorbed dose in the thyroid was computed similarly, using appropriate thyroid absorbed dose rate coefficients. The integration periods were selected to represent the effect of exposure during 1 and 10 years after the accident as well as during a lifetime, which was defined as the time from the beginning of the exposure to age 80. That is, for the three selected age groups, i.e., 1 and 10-year-old children, and 20-year-old adults, the lifetime integration periods were 79, 70 and 60 years, correspondingly.

II. RADIATION MONITORING OF AMBIENT DOSE RATES IN JAPAN SINCE THE ACCIDENT

8. The earlier assessments of external exposures after the accident at FDNPS [UNSCEAR, 2014; WHO, 2012; WHO, 2013] were largely based on previous experience gathered from radioecological and dosimetric studies after global fallout and the Chernobyl accident. Climate, landscape, soil and vegetation types, population density, land use, agricultural practice, diet and lifestyle in Japan differ significantly from those in the previous studies. Different physico-chemical properties of the released and deposited radioactive material, especially different particulate forms affecting mobility or solubility, also contributed to the specificity of the post-accidental situation in Japan.

9. Following the FDNPS accident, extensive monitoring had been undertaken in Japan targeting systematic characterization of the concentrations of radionuclides in the natural, semi-natural and anthropogenic environments. A summary of this monitoring can be found in the recent review [Saito et al., 2019b] as well as in section II.B of appendix A of this UNSCEAR report. The extensive databases gathered due to these monitoring programmes provided substantial empirical evidence and allowed checks to be made of the plausibility and validity of the methods used for external dose assessment. At the same time these data were used to establish and justify alternative assessment methods better suited for characterization of the Japan-specific situation.

10. The methods applied for monitoring of the ambient dose rates in Japan varied greatly, from stationary monitoring, sampling and in-situ measurements to surveys conducted with mobile (air- and car-borne surveys) or portable (walk survey) instruments. All methods were applied systematically and repeatedly thus allowing the creation of a detailed time- and spatial-distribution of ambient dose rate and deposition densities of radionuclides released during the accident.

11. Two types of data were especially useful: firstly, data on deposition density and isotopic composition of radionuclides at specified fixed locations; and, secondly, the observed time dependence of ambient dose rates in various environments including populated areas. The latter were used to check model assumptions for those parameters governing the environmental behaviour of radionuclides on the ground; these undergo radioactive decay, redistribution due to processes of migration in soil, weathering, runoff and human activities, including agricultural and industrial practices as well as decontamination and remediation activities.

III. REVISION OF THE DOSE ASSESSMENT METHODOLOGY FOR M2020

A. Motivation

12. Following the UNSCEAR 2013 Report [UNSCEAR, 2014], substantial changes occurred in Japan with regard to the accumulation of data and understanding the impact of the FDNPS accident on the population and the environment. New data have been obtained and analyses made of: (a) radionuclide concentrations in the environment; (b) the dynamics of ambient dose rates and radionuclide behaviour in the environment; (c) active and extensive monitoring and remediation activities, complemented by improvement of the radiological situation; and (d) return of people to previously evacuated places. The studies undertaken in Japan since 2011 have shown a high degree of compatibility with previous scientific findings from decades of research undertaken globally; but also significant differences in some Japan-specific circumstances. Additionally, new dosimetric data and models, recommended by ICRP [ICRP, 2020], have become available for the assessment of external doses following an accident.

13. An improved, Japanese-specific model for estimating external doses from deposited radionuclides, hereafter referred to as M2020, has been developed to take account of these new data and related developments and is described below.

B. The computational schema

14. The computational schema adopted for M2020 remains essentially the same as that in the UNSCEAR 2013 Report [UNSCEAR, 2014] and can be described by the following equation similar to equation A-1.1 above:

$$\dot{D}(t|a) = r(t)A_{\text{Cs-137}} \sum_m \rho_m e^{-\lambda_m t} \dot{d}_m(a+t) \sum_j f_j(t) p_j(a+t) \quad (\text{A-1.2})$$

where $\dot{D}(t|a)$ is either effective or organ equivalent dose rate for an individual of age a at the beginning of exposure; $\rho_m = \frac{A_m}{A_{\text{Cs-137}}}$ is the ratio of deposition density of the radionuclide m to that of ^{137}Cs on 15 March 2011 (unitless); $\dot{d}_m(a+t)$ is the corresponding age-dependent dose rate coefficient for radionuclide m including also the effect of its radioactive progeny; $p_j(a+t)$ is the fraction of time spent by the individual of age $a+t$ in the location j ; the other parameters remain unchanged and have the same meanings as in equation A-1.1.

C. Radionuclide composition of the deposited radioactive material

15. The calculation of external doses was performed using population-weighted average deposition densities of radionuclides. The data were based on environmental monitoring and were structured in a similar manner to that in the UNSCEAR 2013 Report [UNSCEAR, 2014]. The detailed information can be found in section II.B of appendix A of this report. The population data used for averaging were taken from the results of the Japan 2010 census [MIC, 2011].

16. The data for 2,148 locations aligned and distributed over a 2-km spatial grid were provided by the Japan Atomic Energy Agency [Saito et al., 2019a]. The data consisted of the measured deposition densities of ^{137}Cs , ^{134}Cs , ^{131}I , $^{110\text{m}}\text{Ag}$, $^{129\text{m}}\text{Te}$, ^{89}Sr , ^{90}Sr , ^{238}Pu , ^{239}Pu and

^{240}Pu . Such detailed data were available for the 59 municipalities of Fukushima Prefecture and for neighbouring prefectures: 23 municipalities of Miyagi Prefecture, 5 municipalities of Yamagata Prefecture, 5 municipalities of Tochigi Prefecture and 6 municipalities of Ibaraki Prefecture. All 2,148 locations had measurements of ^{137}Cs deposition density. However, measured deposition densities for other radionuclides were not available for all locations.

17. The data set of deposited radionuclides for each municipality was further modified. First, for 799 data points the concentration of ^{131}I was reconstructed from measurements of ^{129}I in the environment [Muramatsu et al., 2015]. The total number of locations with ^{131}I deposition density levels was 1,297, of which 799 were based on the ^{129}I measurements. When both measured and reconstructed estimates were available at the same location, the reconstructed value was adopted as potentially more accurate.

18. As in the UNSCEAR 2013 Report [UNSCEAR, 2014], the measured deposition densities of shorter-lived radionuclides were not available in all locations. Where measurements were lacking, the deposition densities were estimated using observed radionuclide ratios [UNSCEAR, 2014] in two geographical areas: the so-called South trace, which was formed on 15 March 2011 mainly due to dry deposition, and the rest of the country [IAEA, 2015d]. The ratios as of 15 March 2011 assumed for deposition densities of radionuclides are shown in table A-1.1 and are, essentially, the same values as used in the UNSCEAR 2013 Report [UNSCEAR, 2014].

Table A-1.1. Initial ratios of deposition density at 15 March 2011 used to calculate values for shorter-lived radionuclides from that of ^{137}Cs

Area	Deposition density relative to that of ^{137}Cs						
	^{137}Cs	^{134}Cs	^{136}Cs	^{131}I	$^{129\text{m}}\text{Te}$	^{132}Te (^{132}I) ^a	$^{110\text{m}}\text{Ag}$
All of Japan excluding the South trace ^b	1.0	1.0	0.17	8.3–37 ^c	1.1–1.9 ^c	7.6–13 ^c	0.0028
The South trace	1.0	1.0	0.17	25–250 ^c	1.7–28 ^c	12–190 ^c	0.0028

^a Deposition density of the daughter ^{132}I was assumed equal to that of the parent ^{132}Te at the time of deposition.

^b The towns of Naraha, Hirono, Yamatsuri, Iwaki City of Fukushima Prefecture, the towns of Kitaibaraki, Takahagi of Ibaraki Prefecture.

^c Non-linear relationships were applied for deposition density ratios. See text, equation A-1.2 and table A-1.2.

19. In M2013, the initial ratios of deposition densities for all radionuclides were assumed to be constant across the selected territories and assessed by simply multiplying the initial deposition density of ^{137}Cs by the respective ratio (see equation A-1.1) [UNSCEAR, 2014]. This approach was also applied in M2020 for $^{134,136}\text{Cs}$ and $^{110\text{m}}\text{Ag}$. For $^{131,132}\text{I}$ and $^{129\text{m},132}\text{Te}$, a different approach was used. Based on measured deposition densities of ^{131}I and $^{129\text{m}}\text{Te}$, phenomenological non-linear approximations were used to estimate deposition densities of these radionuclides for locations without measured data, both in the South trace and in the rest of Japan. These measured and approximated values were used for calculation of external doses in populated areas.

20. The initial deposition densities of ^{131}I and $^{129\text{m}}\text{Te}$ plotted versus the initial deposition density of ^{137}Cs are shown in figures A-1.I and A-1.II; the red dots and lines represent data for the South trace and the blue dots and lines represent data for the rest of Japan. Despite their high variability, the data points for the two areas seem to systematically differ from each other; especially, when plotted on log-log scale. For $^{129\text{m}}\text{Te}$, this effect is more pronounced. A simple linear approximation of the log-transformed data resulted in the following phenomenological non-linear approximation for deposition density ratios of either ^{131}I or $^{129\text{m}}\text{Te}$ to that of ^{137}Cs :

$$\rho_x = a A_{\text{Cs-137}}^b \quad (\text{A-1.3})$$

where x stands for either ^{131}I or $^{129\text{m}}\text{Te}$, $A_{\text{Cs-137}}$ is the initial deposition density of ^{137}Cs (kBq/m^2), and the coefficients a and b (unitless), obtained via a non-linear model fit, are shown in table A-1.2. Shaded areas in figures A-1.I and A-1.II indicate the 95% confidence interval of the fit, defined by the uncertainty of the fitted parameters, not the prediction confidence interval that represents the sample variance. The results of the fit suggest different regression slopes for the data for the South trace and for the rest of Japan. Consequently, a straightforward extrapolation of the approximation (equation A-1.3) beyond the range supported by the data may result in an underestimation, for the South trace for high values of ^{137}Cs deposition density. Therefore, for practical application, it has been assumed that the maximum of the two values of the deposition density ratio calculated for the South trace and for the rest of Japan should be used for locations within the South trace. The applicability ranges of equation A-1.3 for different radionuclides and geographical areas are also shown in table A-1.2.

Table A-1.2. Parameters of non-linear relationships between deposition densities of ^{131}I , $^{129\text{m}}\text{Te}$ and ^{137}Cs (see equation A-1.3)

Radionuclide	Area	N	Parameters in equation A-1.3		Applicable in range $A_{\text{Cs-137}}$ (kBq/m^2)
			a	b	
^{131}I	The South trace	232	339.6	-0.473	2–250
	Rest of Japan	1 064	37.31	-0.163	1–10 000
$^{129\text{m}}\text{Te}$	The South trace	304	22.02	-0.441	0.6–320
	Rest of Japan	898	1.865	-0.059	1–10 000

Figure A-1.I. Relationship between deposition densities of ^{137}Cs and ^{131}I for the sampling locations in the South trace (red dots) and in the rest of the country (blue dots). Corresponding phenomenological approximations fitted using equation A-1.3 are shown as lines and their 95% confidence intervals are indicated by the shaded areas

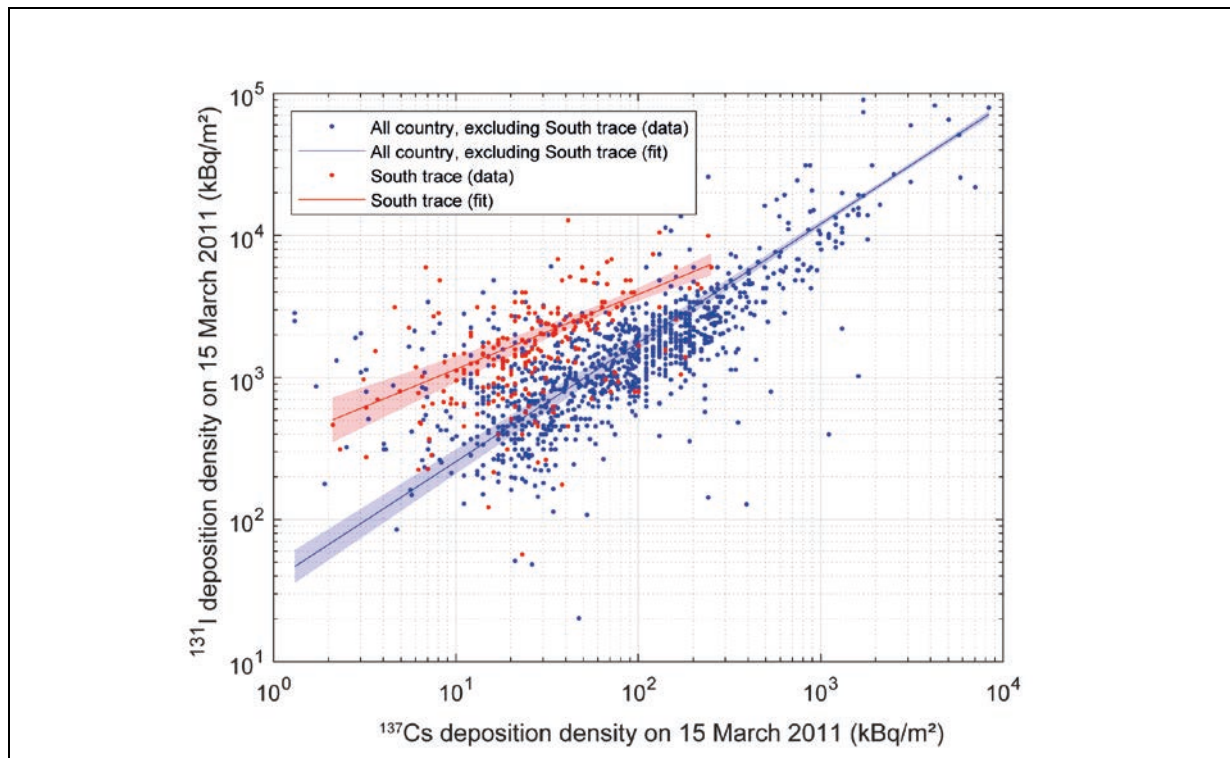
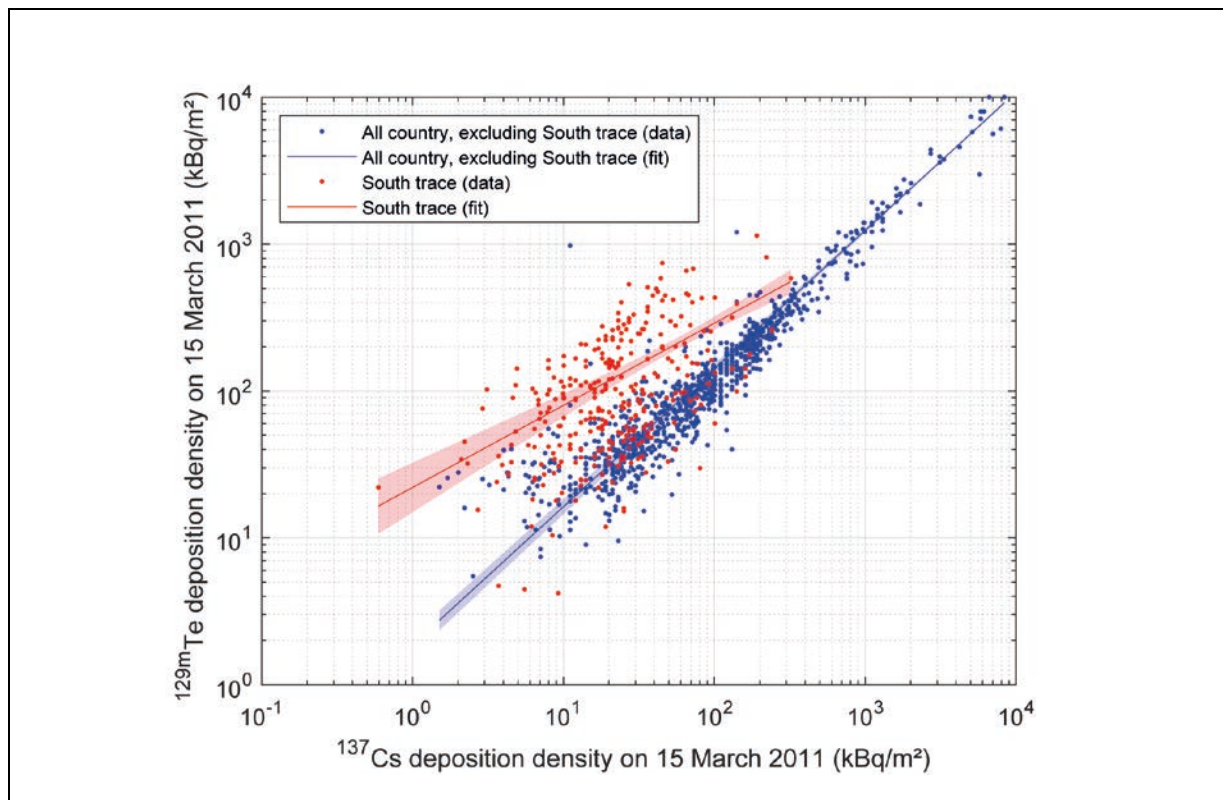


Figure A-1.II. Relationship between ^{137}Cs and $^{129\text{m}}\text{Te}$ deposition densities for sampling locations in the South trace (red dots) and the rest of the country (blue dots). Corresponding phenomenological approximations fitted using equation A-1.3 are shown as lines and their 95% confidence intervals are indicated by the shaded areas



21. The radionuclides shown in table A-1.3 were considered as contributors to external exposure from radioactive material deposited on the ground. For these radionuclides, the contribution of radioactive progeny has been either assumed to be in secular equilibrium or ignored due to their low decay energy yield or high mobility and removal from the environment (noble gases).

22. External doses for remote prefectures were estimated from the deposition density of ^{137}Cs and the deposition density ratios of each radionuclide at a representative location in each prefecture.

Table A-1.3. Properties of the radionuclides deposited on the ground and their radioactive progeny [ICRP, 2008]

<i>Parent radionuclide</i>		<i>Radioactive progeny</i>			<i>Equilibrium applicable?</i>	<i>Negligible?</i>
<i>Name</i>	<i>Half-life (d)</i>	<i>f (%)</i>	<i>Name</i>	<i>Half-life (d)</i>		
$^{110\text{m}}\text{Ag}$	249.8	1.36	^{110}Ag	2.847×10^{-4}	yes	
$^{129\text{m}}\text{Te}$	33.6	64	^{129}Te	0.048	yes	
		36	^{129}I	5.734×10^9	no	Yes ^a
^{132}Te	3.204	100	^{132}I	0.096	yes	
^{131}I	8.021	1.18	$^{131\text{m}}\text{Xe}$	11.84	no	Yes ^b
^{132}I	0.096		none			
^{133}I	0.867	2.89	$^{133\text{m}}\text{Xe}$	2.19	no	Yes ^b
		97.11	^{133}Xe	5.243	no	Yes ^b

Parent radionuclide		Radioactive progeny			Equilibrium applicable?	Negligible?
Name	Half-life (d)	f (%)	Name	Half-life (d)		
¹³⁴ Cs	754.2		none			
¹³⁶ Cs	13.16		none			
¹³⁷ Cs	1.102×10 ⁴	94.40	^{137m} Ba	1.772×10 ⁻³	yes	

^a Contribution to dose is negligible due to long half-life and low energy yield [ICRP, 2008].

^b Noble gas with fast removal.

D. Dose rate coefficients for external exposure from radioactive material deposited on the ground

23. The recent ICRP Publication 144 [ICRP, 2020] provided a comprehensive set of dose rate coefficients for external exposure to environmental sources. It presented dose rate coefficients for air kerma, ambient dose equivalent and effective dose as well as equivalent organ doses for six ages and both sexes (only adults). For ground sources, the radionuclides were considered to be in the form of planar sources located at various depths in soil and volume sources exponentially distributed in soil depth with relaxation mass per unit area ranging from 0.5 to 100 g/cm².

24. Similar to the approach used in M2013, the “effective” planar source at mass depth 0.5 g/cm², combined with the phenomenological function $r(t)$ (see equations A-1.1 and A-1.4), was taken as the basis for calculating external doses after the accident.

25. Values of the free-in-air kerma rate \dot{K}_{air} coefficients ($\mu\text{Gy/h}/(\text{MBq/m}^2)$) and the ambient dose equivalent rate $\dot{H}^*(10)$ coefficients ($\mu\text{Sv/h}/(\text{MBq/m}^2)$) at a height of 1 metre above the ground from an infinite planar radionuclide source located in soil at a mass depth of 0.5 g/cm² for the list of radionuclides in table A-1.3 are shown in table A-1.4, where the dose rate coefficients are for an equilibrium mixture of the parent and the daughter radionuclides.

Table A-1.4. Free-in-air kerma rate coefficients and ambient dose equivalent rate coefficients for an infinite planar radionuclide source at a depth of 0.5 g/cm² in soil [ICRP, 2020]

Radionuclide ^a	\dot{K}_{air} ($\mu\text{Gy/h}/(\text{MBq/m}^2)$)	$\dot{H}^*(10)$ ($\mu\text{Sv/h}/(\text{MBq/m}^2)$)
^{110m} Ag+	8.25	10.0
^{129m} Te+	0.24	0.30
¹³² Te+	7.56	9.43
¹³¹ I	1.17	1.57
¹³² I	6.87	8.45
¹³³ I	1.87	2.37
¹³⁴ Cs	4.78	5.92
¹³⁶ Cs	6.28	7.70
¹³⁷ Cs+	1.75	2.17

^a The “+” sign indicates that the dose coefficient includes a contribution from radioactive progeny under equilibrium conditions.

26. The ICRP Publication 144 [ICRP, 2020] is the first to present ICRP-recommended effective dose rate coefficients for radionuclide sources in soil. Following the general ICRP methodology [ICRP, 1975; ICRP, 1996; ICRP, 2002; ICRP, 2010] and the tissue weighting

factors [ICRP, 2007], the new ICRP effective dose rate coefficients are given for six reference ages for an infinite planar radionuclide source at a mass depth of 0.5 g/cm² in table A-1.5.

Table A-1.5. Effective dose rate coefficients for an infinite planar source at a mass depth of 0.5 g/cm² in soil [ICRP, 2020]

Radionuclide ^a	Effective dose rate \dot{E} ($\mu\text{Sv/h}/(\text{MBq}/\text{m}^2)$) for					
	Newborn	1 year	5 years	10 years	15 years	Adult
^{110m} Ag+	8.79	7.88	7.28	6.72	6.30	6.10
^{129m} Te+	0.23	0.21	0.19	0.17	0.16	0.15
¹³² Te+	7.97	7.14	6.60	6.05	5.66	5.47
¹³¹ I	1.23	1.10	1.02	0.93	0.86	0.83
¹³² I	7.29	6.53	6.03	5.54	5.19	5.03
¹³³ I	1.97	1.77	1.63	1.49	1.39	1.35
¹³⁴ Cs	5.04	4.51	4.16	3.82	3.58	3.47
¹³⁶ Cs	6.70	6.01	5.55	5.13	4.82	4.64
¹³⁷ Cs+	1.83	1.63	1.51	1.38	1.29	1.26

^a The "+" sign indicates that the effective dose rate coefficient includes a contribution from radioactive progeny under equilibrium conditions.

27. ICRP Publication 144 also presents sex-specific organ equivalent dose rate coefficients ($\mu\text{Sv/h}/(\text{MBq}/\text{m}^2)$), which for low-LET photon and electron sources can be regarded as numerically equal to the absorbed dose rate coefficients. In the present report, these dose rate coefficients have been used to calculate doses for the following organs: colon, red bone marrow, thyroid and female breast. The age-dependent thyroid equivalent dose rate coefficients are shown in table A-1.6 (male) and in table A-1.7 (female).

Table A-1.6. Thyroid equivalent dose rate coefficients for males for an infinite planar source at a mass depth of 0.5 g/cm² in soil [ICRP, 2020]

Radionuclide ^a	Thyroid equivalent dose rate ($\mu\text{Sv/h}/(\text{MBq}/\text{m}^2)$) for male					
	Newborn	1 year	5 years	10 years	15 years	Adult
^{110m} Ag+	9.05	7.62	7.19	6.57	6.41	6.36
^{129m} Te+	0.23	0.19	0.19	0.17	0.16	0.16
¹³² Te+	8.27	6.83	6.48	5.95	5.75	5.71
¹³¹ I	1.30	1.02	1.00	0.90	0.86	0.86
¹³² I	7.54	6.25	5.90	5.44	5.28	5.23
¹³³ I	2.05	1.66	1.59	1.46	1.42	1.40
¹³⁴ Cs	5.23	4.29	4.05	3.76	3.64	3.60
¹³⁶ Cs	6.89	5.83	5.54	5.02	4.88	4.83
¹³⁷ Cs+	1.91	1.55	1.46	1.37	1.32	1.30

^a The "+" sign indicates that the dose rate coefficient includes a contribution from radioactive progeny under equilibrium conditions.

Table A-1.7. Thyroid equivalent dose rate coefficients for females for an infinite planar source at a depth of 0.5 g/cm² in soil [ICRP, 2020]

Radionuclide ^a	Thyroid equivalent dose rate ($\mu\text{Sv/h}/(\text{MBq}/\text{m}^2)$) for female					
	Newborn	1 year	5 years	10 years	15 years	Adult
^{110m} Ag+	9.18	7.82	7.32	6.64	6.51	6.21
^{129m} Te+	0.24	0.19	0.19	0.17	0.17	0.16
¹³² Te+	8.38	7.00	6.62	5.97	5.89	5.63
¹³¹ I	1.33	1.04	1.02	0.90	0.89	0.88
¹³² I	7.64	6.42	6.03	5.47	5.39	5.14
¹³³ I	2.09	1.70	1.62	1.47	1.44	1.41
¹³⁴ Cs	5.30	4.41	4.15	3.77	3.73	3.56
¹³⁶ Cs	6.99	5.96	5.62	5.07	4.97	4.74
¹³⁷ Cs+	1.93	1.59	1.50	1.37	1.35	1.29

^aThe “+” sign indicates that the dose rate coefficient includes a contribution from radioactive progeny under equilibrium conditions.

E. Dynamics of ambient dose rates due to downward migration and weathering

28. The effect of natural processes, resulting in the redistribution of radionuclides in undisturbed areas and the corresponding reduction of the ambient dose rates in air, was accounted for in a similar manner to that in M2013, i.e., via an empirical reduction function $r(t)$ applied to the dose rates from a planar source in soil at a mass depth of 0.5 g/cm², which effectively approximates dose rates from freshly deposited radionuclides [Jacob et al., 1986; Jacob and Paretzke, 2017; Petoussi-Henss et al., 2012]. Conventionally, the reduction function $r(t)$ is approximated by a pragmatic two-exponential expression with empirically defined parameters:

$$r(t) = Ae^{-\frac{\ln 2}{T_A}t} + Be^{-\frac{\ln 2}{T_B}t} \quad (\text{A-1.4})$$

where t is the time since the accident (year); typically, the coefficients A and B add up to 1 and represent relative weights of the two, fast and slow, processes characterized by their respective half-lives T_A and T_B (year). In M2013 [UNSCEAR, 2014], derived from the Chernobyl-based studies [Golikov et al., 2002; Jacob, 1996; Likhtarev et al., 2002], the parameters $A = B = 0.5$ were selected and the half-lives for the fast and the slow components were 1.5 and 50 years, respectively.

29. Since the publication of the UNSCEAR 2013 Report [UNSCEAR, 2014], further extensive monitoring has been undertaken in Fukushima Prefecture and the neighbouring prefectures. This has provided a means for checking the assumed phenomenological relationships over a period of several years of observations. Specifically, for the reduction function $r(t)$, the data reported by Mikami et al. [Mikami et al., 2019] for fixed undisturbed locations, mostly in populated areas, have been used in combination with the earlier data from studies of global fallout in Europe and North America [Miller et al., 1990; Schimmack et al., 1998]. These data, corrected for the ratios of caesium isotopes and their decay to express a net effect of downward migration, weathering and runoff, were fit by the two-exponential function (equation A-1.4), resulting in the following parameters (see equation A-1.5):

$$A = 0.37, T_A = 2.8 \text{ year}, B = 0.63, T_B = 20.7 \text{ year} \quad (\text{A-1.5})$$

30. The data and the model estimates using the M2013 and M2020 parameters are shown in figure A-1.III. The 95% confidence interval of the fit is indicated by a blue shaded area.

31. Also plotted in figure A-1.III is the reduction function computed using the dose rate coefficients [ICRP, 2020] for a more realistic radionuclide source exponentially distributed in the soil depth, whose relaxation mass per unit area gradually changes with time (see e.g., [Minenko et al., 2006]). Mikami et al. [Mikami et al., 2019] reported values of the “effective” relaxation mass per unit area β_{eff}^2 based on the successive observations made in the undisturbed sites, mostly in populated areas of the 80-km zone around FDNPS, covering a period from late 2011 to 2017; their data suggest a linear approximation for the relaxation mass per unit area:

$$\beta(t) = \beta_0 + v_\beta t \quad (\text{A-1.6})$$

with the following parameters: $\beta_0 = 0.8 \text{ g/cm}^2$ and $v_\beta = 0.415 \text{ (g/cm}^2\text{)/year}$.

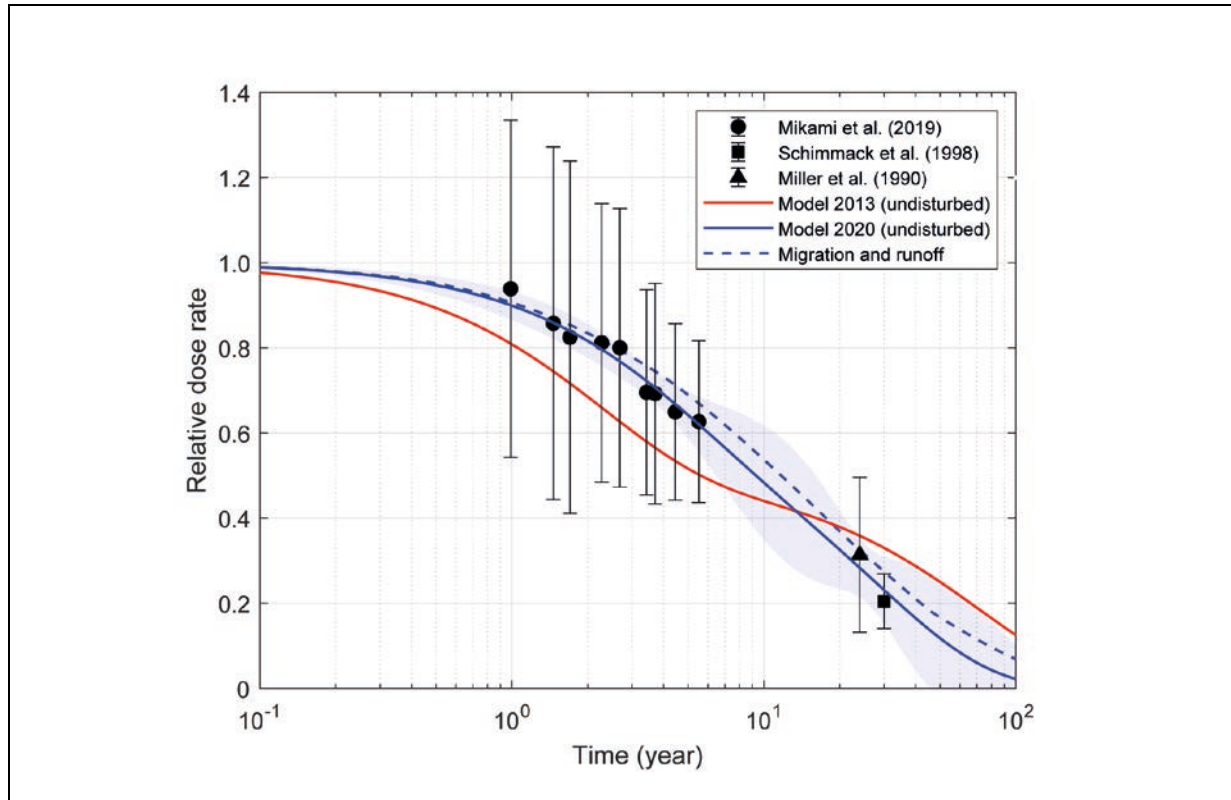
32. Comparison of the empirical reduction function (equations A-1.4 and A-1.5) and the dose reduction assessed for an exponential source in soil using the time-dependent relaxation mass per unit area (equation A-1.6) shows good agreement, especially, in the late period where no Japan-specific data exist yet (see figure A-1.III). Based on this observation, the empirical function (equation A-1.4) with the parameters (equation A-1.5) had been regarded as a plausible approximation of the trend in the future dose reduction and was, therefore, applied in the external dose calculations to approximate dose reduction due to natural processes on undisturbed land in populated areas.

33. As seen from figure A-1.III, the variant of the empirical reduction function (equation A-1.4) used in the UNSCEAR 2013 Report [UNSCEAR, 2014] results in a faster dose reduction for 15 years following the accident. The phenomenon of slower dose reduction due to natural redistribution of radionuclides in Japan following the FDNPS accident was explicitly addressed by Saito et al. [Saito et al., 2019b]. It was identified as one of the specific features of the post-accident situation in Japan that required critical evaluation with implications for the external dose assessment methodology.

² “Effective” relaxation mass per unit area β_{eff} is defined [Mikami et al., 2019; Saito et al., 2019a] as the parameter of an exponential distribution in soil which results in the same absorbed dose rate at 1 metre above the ground as the real source of the same inventory (integral deposit).

Figure A-1.III. Reduction of the dose rate in air above undisturbed ground due to downward migration in soil, weathering and runoff

Points represent results derived from environmental measurements of Mikami et al. [Mikami et al., 2019] (solid circles), Schimmack et al. [Schimmack et al., 1998] (solid square) and Miller et al. [Miller et al., 1990] (solid triangle). The lines show phenomenological functions used in the UNSCEAR 2013 Report [UNSCEAR, 2014] (red solid line) and fitted to the data (blue solid line) as well as the dose rate reduction for time-dependent exponential source in soil with weathering and runoff (dashed blue line). The blue shaded area indicates 95% confidence interval for the fitted curve



F. Dynamics of ambient dose rates in populated areas

34. Dose rates in air above contaminated ground in populated and, especially, in urban areas are known to be less than those observed at the same time in virgin or undisturbed environments [Eged et al., 2006; Golikov et al., 2002; Jacob and Meckbach, 1987; Jacob, 1996; Likhtarev et al., 2002; Meckbach and Jacob, 1988; UNSCEAR, 2014]. Extensive and systematic monitoring activities were undertaken in Japan after the accident using airborne and car-borne radiation monitoring surveys as well as those on foot [Andoh et al., 2018a; Andoh et al., 2018b; Kinase et al., 2017; Mikami et al., 2019; Saito et al., 2019a]. The comprehensive analysis by Saito et al. [Saito et al., 2019b] revealed systematic differences between the various monitoring methods, probably reflecting the fact that: (a) airborne observations were providing dose response averaged over larger areas and different landscapes; (b) car-borne surveys were largely constrained to roads and paved surfaces; and (c) surveys on foot included paved roads and streets, residential areas with more unpaved areas, etc. Correspondingly, as shown in Saito et al. [Saito et al., 2019b], the airborne (helicopter-based) measurements demonstrated the slowest reduction in dose rates with time, similar or even slower than observed at fixed location (mostly undisturbed) sites. The car-borne surveys showed the fastest dose rate reduction, with the data from surveys carried out on foot intermediate between the car-borne and the fixed location measurements.

35. M2013 [UNSCEAR, 2014] was largely based on Chernobyl experience in environments significantly different from those in the affected areas of Japan. Consequently, its use in Japan may have resulted in some systematic over- or underestimation of doses from external exposure.

36. Mountainous forest landscape of the affected parts of Fukushima Prefecture, higher population density and almost all flatland being used or involved in anthropogenic activities as well as urbanized populated areas determine specificities of the post-accidental situation in Japan. To evaluate the implications of these specificities, the data from the car-borne surveys [Andoh et al., 2018a] were analysed and compared to location factors from M2013 for paved and unpaved surfaces in outdoor locations.

37. Data for the reduction in the external dose rate (solid symbols) derived from the car-borne surveys are shown in figure A-1.IV [Andoh et al., 2018a; Kinase et al., 2017], with the effect of radioactive decay removed. The lines in figure A-1.IV represent model calculations based on dose rate reduction due to downward migration into the soil (see equation A-1.4) with various parameters and the additional location factors for non-natural surfaces. M2013 estimates are for paved and unpaved surfaces and are shown as red solid and red dashed lines, respectively. The blue solid line in the figure represents the dose rate reduction obtained from a fit to the car-borne data and uses the following location factors for road and streets:

$$f_{\text{roads}}(t) = 0.30 \exp\left(-\frac{\ln 2}{0.95} t\right) + 0.65 \quad (\text{A-1.7})$$

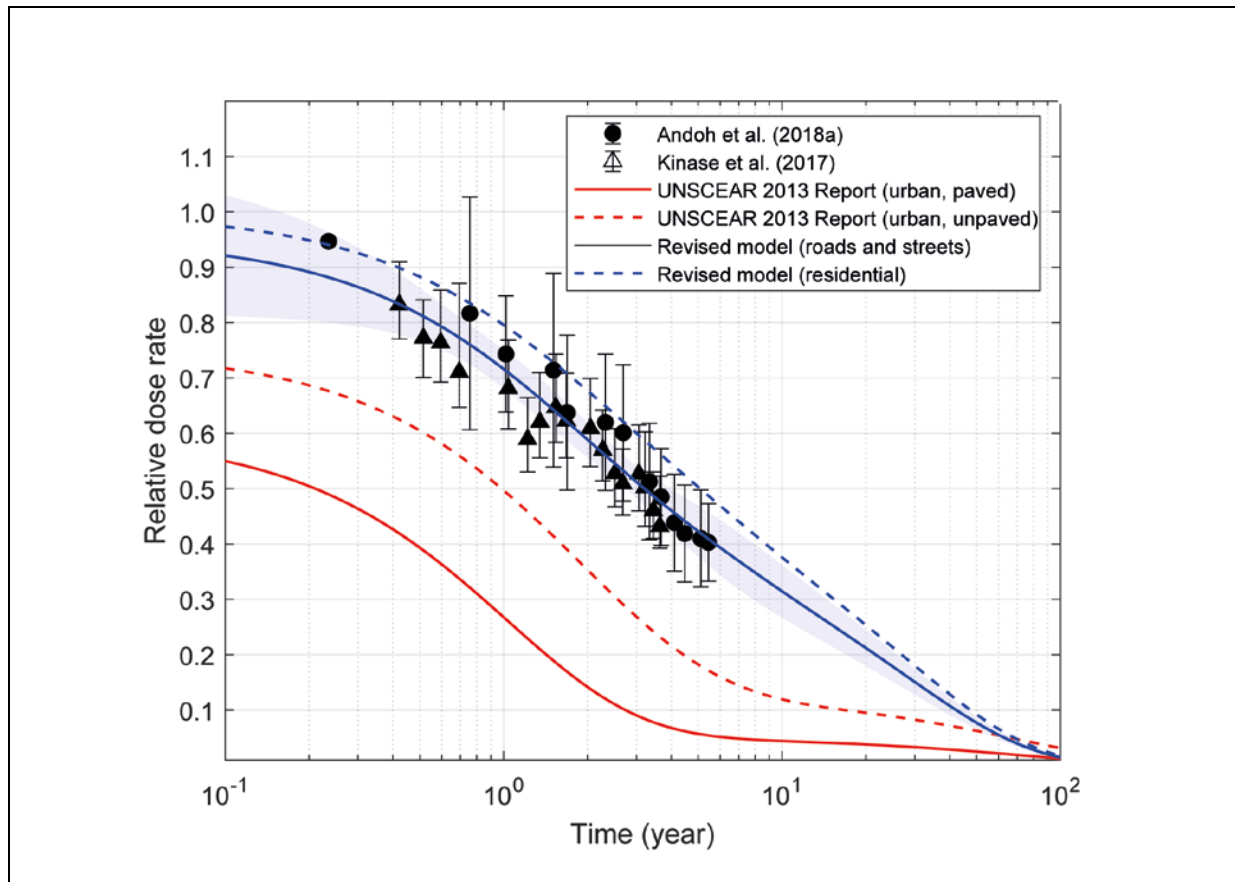
where time t is in years. The blue shaded area represents the 95% confidence interval of the fitted approximation (equation A-1.7) due to uncertainty in the parameters.

38. For residential areas, the location factor was derived using the observations of Andoh et al. [Andoh et al., 2018b] who demonstrated that the data from surveys carried out on foot, collected in the period 2.3–5.7 years after the accident, showed higher dose rates than observed in the car-borne surveys in the same areas by 20% on average, ranging from +13% at higher dose rates ($>1 \mu\text{Sv/h}$) to +30% at lower dose rates ($<1 \mu\text{Sv/h}$). The following approximation was selected for M2020 to represent such behaviour in residential areas:

$$f_{\text{residential}}(t) = 0.22 \exp\left(-\frac{\ln 2}{0.95} t\right) + 0.78 \quad (\text{A-1.8})$$

where t is in years and the resulting dose rate reduction factor is shown in figure A-1.IV as the blue dashed line.

Figure A-1.IV. The external dose rate reduction factors for paved areas in populated places as: (a) derived from the car-borne surveys [Andoh et al., 2018a; Kinase et al., 2017] and shown as solid symbols; (b) calculated using M2013 (red lines); and (c) fitted to the data and implemented in M2020 (blue lines). The blue shaded area indicates 95% confidence interval for the fitted curve



G. Shielding factors for houses

39. Unlike in M2013, where the indoor location factors had their own time dependence, in M2020 the location factors $f_j(t)$ for indoor locations have been obtained as a product of the location factor for residential areas (equation A-1.8) and a constant shielding factor, representing the effect of reduction of the anthropogenic dose inside houses. The same types of house were considered as in the UNSCEAR 2013 Report: a wooden house, a wooden fireproof house and a concrete house or building. For these house types, the shielding factors were assumed to be the same as in M2013: 0.4 for wooden houses, 0.2 for wooden fireproof houses, and 0.1 for concrete buildings. These values are based on the earlier experience and studies [Golikov et al., 2002; Likhtarev et al., 2002; Meckbach and Jacob, 1988; UNSCEAR, 2014] and also consistent with the recent observations made by the Japanese authors; e.g., Matsuda et al. [Matsuda et al., 2017] reported shielding factors for one- and two-storey wooden or light-steel frame houses to be in range from 0.38 to 0.49, while their data also suggested that shielding factors for the concrete buildings would not exceed 0.15.

H. Fractions of time spent in various locations (occupancy factors)

40. Papers published since 2013 in peer-reviewed journals have presented deterministic estimates of annual occupancy factors for four age-social groups of Japanese people; some of them were derived from the official sources of the national population statistics [MIC, 2017].

The summary in table A-1.8 contains arithmetic means (AM) of fractions of time $p_j(a + t)$ spent by various social groups of adult Japanese people and children of various ages in different exposure conditions.

Table A-1.8. Fractions of time (occupancy factors) spent in various locations by different population groups

Type of location	Fraction of time for the population group				
	Children		Adult workers		Retired ^a
	1 year	10 year	Outdoor	Indoor	
Indoors, including:	0.9	0.9	0.7	0.9	0.9
At home and others	0.7	0.7	0.7	0.6	0.9
At work, school, kindergarten, etc.	0.2	0.2		0.3	
Outdoors, including:	0.1	0.1	0.3	0.1	0.1
Residential areas	0.1	0.1	0.2	0.1	0.1
Unpaved surfaces			0.1		

^a Exposure conditions and external doses for retired people are similar to those for indoor workers.

41. The data collected mostly in Fukushima Prefecture do not contradict the national statistical data provided by the Statistics Bureau of Japan.³ Neither summarized papers nor data presented by the Statistics Bureau of Japan contain explicit values for time spent by various groups of people indoors and outdoors. However, these have been estimated indirectly from the data presented above.

42. Deterministic estimates of external doses have been made for the following four social/age groups:

- A 1-year-old infant as a representative for the group of preschool children (those aged 0–5 years in March 2011);
- A 10-year-old child as a representative for the group of school children (those aged 6–15 years in March 2011);
- A 20-year-old adult as a representative for the group of adults (those aged 16 and older in March 2011) who work mostly indoors, including students and pensioners;
- A 20-year-old adult as a representative for the group of adults (those aged 16 and older in March 2011) who work mostly outdoors.

43. Explicit consideration has not been given to retired people as a group; their doses will be broadly comparable to those for indoor workers.

44. According to Japanese national statistics [MIC, 2015], the majority of the population of Fukushima Prefecture and neighbouring prefectures reside in wooden or wooden fireproof one-to-two-storey houses. Therefore, in M2020 it is assumed for all age-social groups of Japanese people that they live (at home and others) in wooden one-to-two-storey houses and work or study (at work, school, kindergarten, etc.) in concrete buildings.

³ See website: [MIC, 2017].

I. Summary of M2020

45. Doses to members of public from exposure to radioactive material deposited in the terrestrial environment following the accident at FDNPS were calculated as follows.

46. Based on the computational schema described above, the integrated doses for various age and social population groups, for evacuees and those returning subsequently to their homes were estimated using the following equation:

$$D(t_1, t_2|a_0) = c \int_{t_1}^{t_2} \dot{D}(t|a_0) dt \quad (\text{A-1.9})$$

where $\dot{D}(t|a_0)$ is the rate of the dose quantity of interest, effective or organ equivalent dose; a_0 is the age when accidental radiation exposure started for the considered population group; times t_1 and t_2 bound the exposure period; and the unit conversion coefficient c depends on the selected dimensions of the quantities used (time, deposition density, dose rate coefficients, decay data, half-lives).

47. The dose rate was evaluated as:

$$\dot{D}(t|a_0) = r(t) A_{\text{Cs-137}} \sum_m \rho_m e^{-\lambda_m t} \dot{d}_m(a+t, s) \sum_j f_j(t) p_j(a+t) \quad (\text{A-1.10})$$

where $A_{\text{Cs-137}}$ is the deposition density of ^{137}Cs on 15 March 2011 (Bq/m^2); $r(t)$ is the empirical two-exponential reduction function (see equation A-1.4) describing dose reduction due to natural processes of redistribution (downward migration, weathering, runoff):

$$r(t) = 0.37 e^{-\frac{\ln 2}{2.8} t} + 0.63 e^{-\frac{\ln 2}{20.7} t} \quad (\text{A-1.11})$$

where t is time since 15 March 2011 (year); ρ_m is the initial ratio of the radionuclide m deposition density to deposition density of ^{137}Cs (unitless); λ_m is the radioactive decay rate of the radionuclide m (1/year); $\dot{d}_m(a+t, s)$ is the dose rate coefficient for an “effective” planar source at a mass depth of $0.5 \text{ g}/\text{cm}^2$ for the radionuclide m and its progeny in equilibrium conditions for a person of age $a+t$ and sex s ($\text{mSv}/\text{year}/(\text{MBq}/\text{m}^2)$); $f_j(t)$ are the locations factors (unitless) defined as follows in equation A-1.12:

$$f_i(t) = \begin{cases} 1, & \text{outdoor, undisturbed areas} \\ \left(0.22 e^{-\frac{\ln 2}{0.95} t} + 0.78\right) \times \begin{cases} 1.0, & \text{outdoor, populated areas} \\ 0.4, & \text{indoor, wooden house} \\ 0.2, & \text{indoor, wooden fireproof house} \\ 0.1, & \text{indoor, concrete house} \end{cases} \end{cases} \quad (\text{A-1.12})$$

$p_j(a+t)$ is the occupancy factor, i.e., fraction of lifetime spent in the location j , for a person of age $(a+t)$ and of a specific occupancy type. The occupancy types considered are those for preschool and school children, outdoor workers, indoor workers and pensioners. The occupancy factors adopted in M2020 have been simplified, compared with those in M2013, and are shown in table A-1.8.

48. The uncertainties in the model estimates were assessed using a Monte Carlo simulation based on equations A-1.9 and A-1.10 and using estimated or implied uncertainties in the area-

averaged values of ^{137}Cs deposition density and other model parameters. Particularly, area-averaged values of ^{137}Cs deposition density were taken as log-normally distributed with an estimated geometric standard deviation (GSD) of 1.5. The dose rate coefficients [ICRP, 2020] were assumed to follow normal distributions with the 95% confidence interval specified by a relative error of 20%. The empirical dose rate reduction function (equation A-1.11) was assumed to be log-normally distributed with a GSD of 1.2 for integration periods of 1 and 10 years after the accident and with a GSD of 1.3 for longer integration periods to address higher uncertainty due to extrapolation of the fitted function beyond the data-supported domain. Deposition density ratios ρ_m (see table A-1.1 and equation A-1.3) were also assumed to be log-normally distributed with a GSD of 1.1 for all radionuclides except for ^{131}I , for which the uncertainty was expressed by a GSD of 1.5 to reflect the higher variability observed in the measured data (see figure A-1.I). Uncertainty specific to location and occupancy factors was evaluated as corresponding to log-normally distributed quantities with a GSD of 1.2, correspondingly, the uncertainty of the combined factor (see inner sum in equation A-1.2) was taken as represented by a GSD of 1.3, assuming statistical independence of both factors. Sample size in the stochastic simulations was chosen equal to 10,000.

49. This Monte Carlo technique was applied to generate samples for different ages, types of occupancy and periods of exposure. The main statistical properties of the generated samples are summarized in table A-1.9. Specifically, the ratios of the estimated geometric mean (GM) and 5th and 95th percentiles to the corresponding AM of a generated distribution were calculated. These ratios for different population groups were found to be very similar, so only the group-averaged values are shown in table A-1.9.

Table A-1.9. Statistical characteristics of uncertainty associated with M2020 estimates of cumulative external doses

<i>Exposure period</i>	<i>5th percentile</i>	<i>GM</i>	<i>AM</i>	<i>95th percentile</i>
1 year	0.54	0.94	1	1.66
10 years	0.54	0.94	1	1.66
Lifetime	0.49	0.93	1	1.76

IV. VALIDATION OF M2020 FOR DOSES FROM EXTERNAL EXPOSURE

50. The validity of external dose estimates made with M2020 was tested by applying the models to the results of the several personal dosimetry surveys performed in Fukushima Prefecture and published in the scientific literature. Based on published data, several validation scenarios were developed and used for comparing the models' predictions and the reported measurements.

A. The Fukushima Health Management Survey (Scenario A)

51. The Fukushima Health Management Survey (FHMS) was undertaken to obtain individualized estimates of population exposure following the FDNPS accident and involved residents of seven areas in Fukushima Prefecture [Akahane et al., 2013; Ishikawa et al., 2015]. The study was essentially a model-based dose reconstruction produced by integration of ambient dose rates, model-simulated and interpolated from measured values, taking into account details of individual behaviour acquired through interviews or questionnaires. The effective doses for the residents of Fukushima Prefecture were reconstructed for the four-month period from 15 March 2011 to 11 July 2011. The model used in the study for external dose calculations was largely compatible to the methodology presented in the UNSCEAR 2013 Report [UNSCEAR,

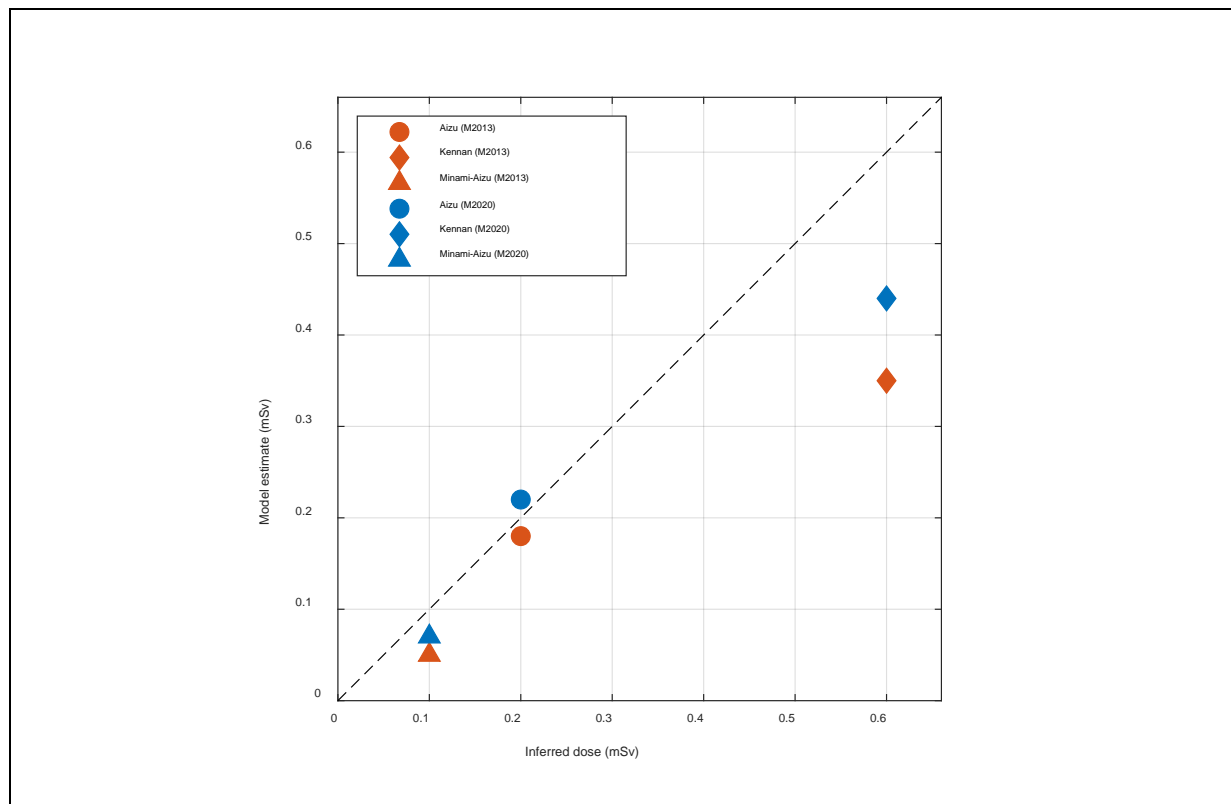
2014], excluding outdoor location factors, which were unnecessary as the ambient dose rates were estimated for living places, while the indoor location factors were conservatively taken as time independent shielding factors.

52. For comparison with dose estimates made using the M2013 and M2020 models, the three areas with non-evacuated populations have been selected: Aizu, Kennan and Minami-Aizu [Ishikawa et al., 2015].

53. The external doses were calculated for exposures to radioactive sources in air (plume) and on the ground for the period from 15 March 2011 to 11 July 2011, accounting for the age- and social population structure as reported by Ishikawa et al. [Ishikawa et al., 2015]. The results were obtained using both the M2013 and M2020 models. Comparison of the area-averaged inferred doses with the model-calculated doses is shown in figure A-1.V.

54. The estimates using the M2013 and M2020 models agree well with the values of external doses inferred in FHMS [Akahane et al., 2013; Ishikawa et al., 2015] for the area Aizu (figure A-1.V, circles). Both models underestimate the FHMS values for Minami-Aizu (figure A-1.V, triangles) by a factor of 1.3–2. However, the absolute difference is small, 0.03–0.05 mSv; in particular, it is less than the assumed natural background dose of 0.086 mSv during the study period, so associated uncertainties are relatively high and the model estimates can be regarded as comparable with the inferred FHMS values. The FHMS values for the Kennan area are larger, by approximately 0.25 mSv for M2013 and 0.16 mSv for M2020; these differences may be attributed to several factors, e.g., differences in the model assumptions and parameters, inherent uncertainties of the atmospheric dispersion models used in FHMS, assumptions on the population structure, lifestyle and dwelling types, underestimation of the contribution from shorter-lived radionuclides.

Figure A-1.V. Comparison of the external effective doses for the period 15 March 2011 to 11 July 2011 inferred from individual questionnaires [Akahane et al., 2013; Ishikawa et al., 2015] and the dose estimates obtained using M2013 [UNSCEAR, 2014] and M2020 models (this UNSCEAR report)



55. For example, the Kennan area includes the Yamatsuri municipality which, in both M2013 and M2020, is assigned to the South trace with a higher contribution of shorter-lived radionuclides, resulting in a net anthropogenic external dose of 0.6 mSv. The municipalities of Samegawa, Hanawa and Tanagura, also belonging to the Kennan area and adjacent to Yamatsuri, are assumed to have radiological conditions typical of the rest of Japan. An alternative assumption, that these municipalities should have been attributed to areas with conditions typical of the South trace, would have increased the M2020 estimates for the whole Kennan area from 0.44 to 0.49 mSv, which is only 20% less than that reported in the FHMS results.

56. The comparison of the FHMS estimates with those based on M2020 cannot be judged as a fully independent objective benchmark, because the estimates are inferred based on various methods and assumptions. More informative comparisons can be made with results of personal dosimetry campaigns conducted in the affected areas.

B. Personal dosimetry studies

57. Following the FDNPS accident, several personal dosimetry campaigns have been and continue to be conducted in Japan and the results of some have been reported in the peer-reviewed literature. These campaigns targeted various areas and were performed over a range of periods of time, seasons and or different population groups.

58. Typically, luminescence dosimeters were distributed among population groups in the study areas. At the end of the study period, the dosimeters were collected and processed. The total, background and anthropogenic, accumulated doses, in terms of the personal dose equivalent, $H_p(10)$, were determined in dosimetry laboratories and the same assumed value of the background dose was subtracted. The net measured dose was often assumed as a proxy for effective dose and, correspondingly, no further conversion was applied to the measured values. In such cases, for comparison with M2013 and M2020 estimates, the reported measured anthropogenic personal equivalent doses were converted to effective dose values for the respective age groups using the conversion coefficients derived by Satoh et al. [Satoh et al., 2017]. The model calculations were performed for specially defined population groups and behavioural patterns selected to match, as closely and reasonably as possible, the study population groups and their living and working conditions.

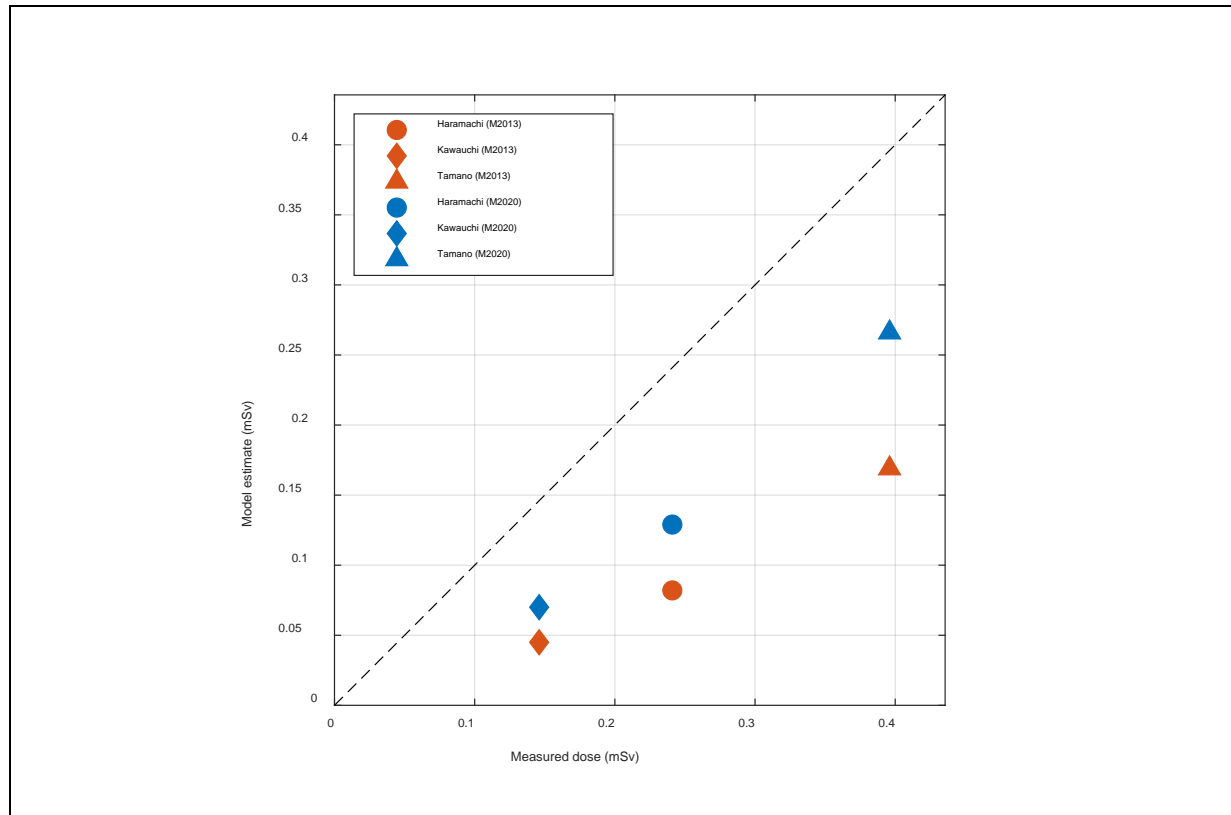
1. Scenario B: Kawauchi, Tamano, Haramachi areas in 2012

59. Scenario B was derived from the personal dosimetry study undertaken in Kawauchi Village, Tamano area (a part of Soma City) and Haramachi area (a part of Minamisoma City) in 2012 [Harada et al., 2014]. The dosimeters were worn for two months from 1 August 2012 to 30 September 2012. The study group consisted of 483 adults. The background dose during the study period was assumed to be 0.1 mSv deduced from the reported pre-accident annual background dose in the range of 0.61–0.63 mSv.

60. The results of the study are compared to the M2013 and M2020 estimates in figure A-1.VI, from which it is seen that the model-calculated values significantly underestimate the values reported by Harada et al. [Harada et al., 2014]. The reason for the systematic differences apparent in figure A-1.VI is unclear and may have several origins. Notably, comparisons with results from other studies for the same areas and time periods (see the following subsections) demonstrate significantly better agreement between the measured and the model-calculated values, suggesting

that there may be an unknown systematic factor influencing the measured values reported by Harada et al. [Harada et al., 2014].

Figure A-1.VI. Comparison of the external effective doses from personal dosimetry data [Harada et al., 2014] and the dose estimates obtained using M2013 [UNSCEAR, 2014] and M2020 models (this UNSCEAR report)



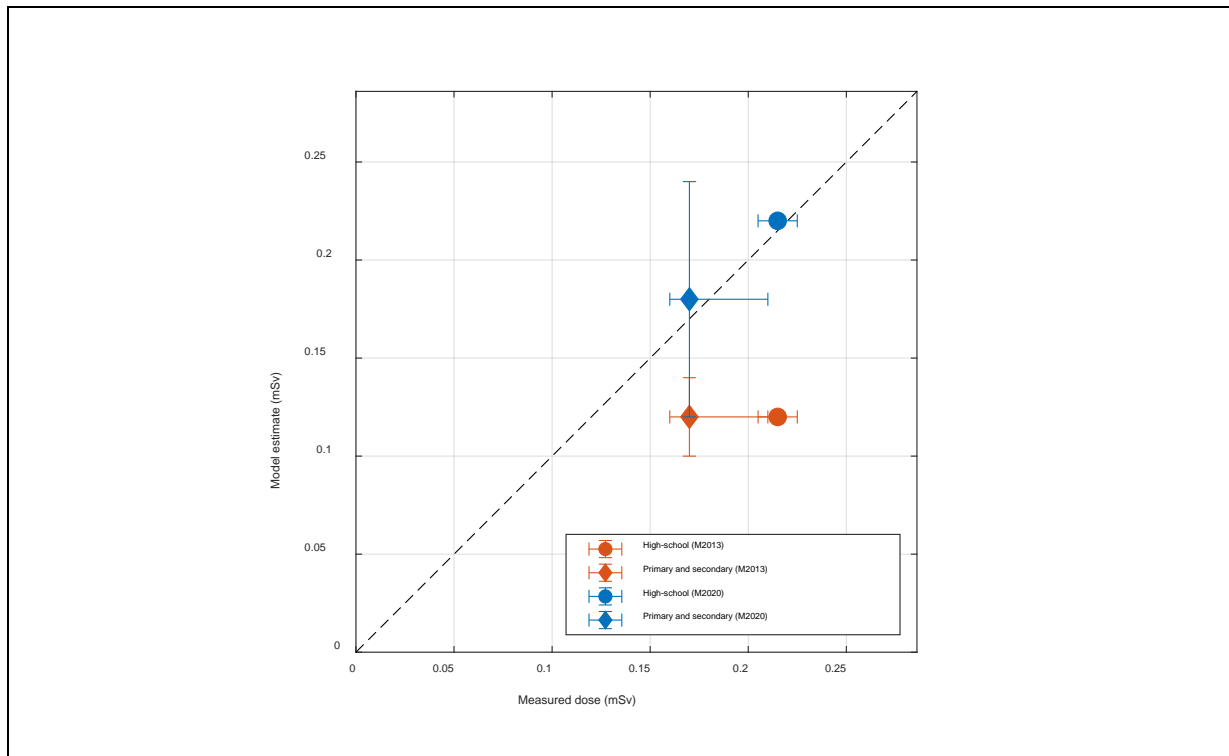
2. Scenario C: Minamisoma City school children in 2012

61. The study selected for this validation scenario was conducted in Minamisoma City among 520 school children during three months in September–November 2012 [Nomura et al., 2015; Nomura et al., 2016]. The children represented various school grades (primary, secondary and high), thus making it possible to compare their doses with the model-estimated doses for 10-year-old children and adults.

62. The reported measured anthropogenic doses were in the range of 0.17–0.22 mSv and are small and close to the assumed background dose 0.14 mSv for the study period, which corresponds to an annual background dose of 0.54 mSv. Therefore, variations in the background about the single value assumed in the study would result in additional unknown uncertainties in the measured values. Indeed, Nomura et al. [Nomura et al., 2015; Nomura et al., 2016] reported part of the measured data to have zero values after subtraction of the assumed background dose.

63. Comparison of the measured and model-calculated external doses is shown in figure A-1.VII, where the error bars indicate ranges of the estimates derived for various ages and housing types. M2013 underestimates the measured values while M2020 is in much better agreement with the measured doses.

Figure A-1.VII. Comparison of the external effective doses from personal dosimetry data for Minamisoma City school children in September–November 2012 [Nomura et al., 2015; Nomura et al., 2016] and the corresponding dose estimates obtained using M2013 [UNSCEAR, 2014] and M2020 models (this UNSCEAR report)



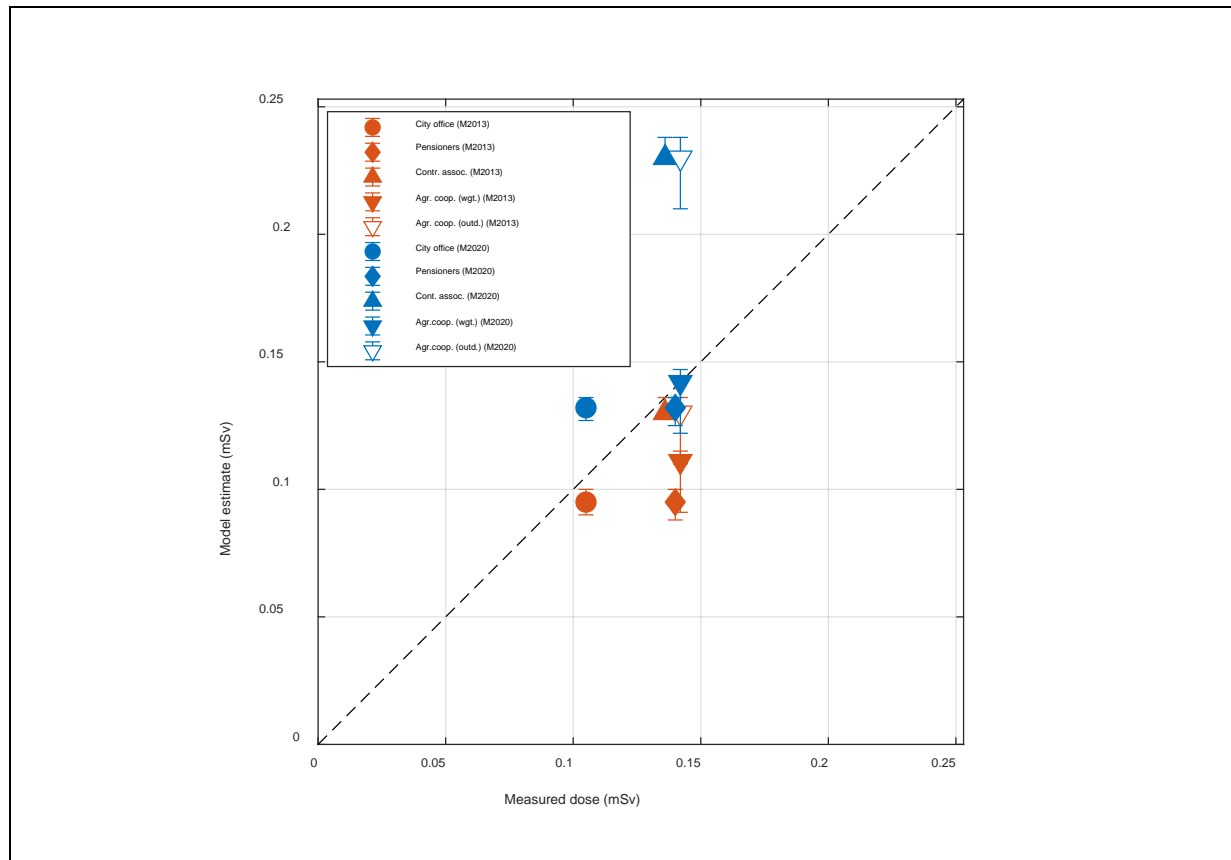
3. Scenario D: Adults in Fukushima City and in the neighbourhood

64. The study was performed during one month in the period February–April 2012 [Takahara et al., 2014] and included 499 adult participants from Fukushima City and neighbouring municipalities comprising: the city office employees, retired persons, members of the contractor association and agriculture cooperatives. The natural background dose was assumed to be 0.05 mSv during the month of the study and was inferred from the reported pre-accident annual background dose of 0.63 mSv.

65. The measured and model-calculated values are compared in figure A-1.VIII. Both models predicted anthropogenic external doses close to those obtained from personal dosimeters. In general, M2020 provides a better fit to the measured doses while M2013 tends to underestimate them.

66. The model calculations for the members of the contractor association and agricultural workers were conservative and based on an assumption that they spent 100% of their working time outdoors. These estimates are shown in figure A-1.VIII as solid upward pointing triangles and empty downward pointing triangles, respectively. M2020 (blue symbols) clearly overestimates the measured doses for these groups. Less conservative M2020 estimates for agricultural workers, assuming their working time is equally shared between indoor and outdoor activities, is shown as solid downward pointing triangle and is in much better agreement with the measurements. This difference demonstrates the effect of uncertainty in the occupancy factors when trying to make valid comparisons between modelled and measured doses.

Figure A-1.VIII. Comparison of the external effective doses from personal dosimetry data for adults in Fukushima City and neighbouring municipalities in February–April 2012 [Takahara et al., 2014] and the corresponding dose estimates obtained using M2013 [UNSCEAR, 2014] and M2020 models (this UNSCEAR report)

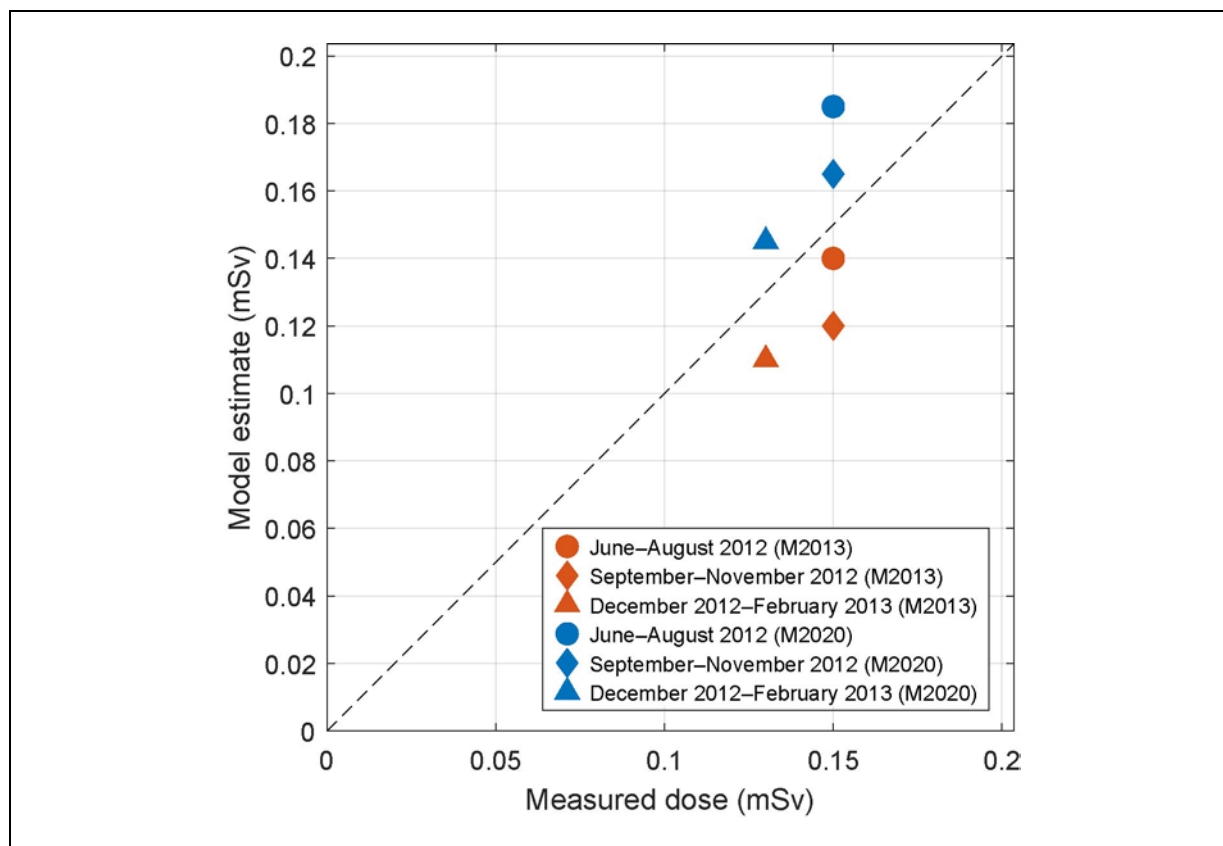


4. Scenario E: Minamisoma City children

67. The study selected for this validation scenario was conducted from June 2012 to February 2013 in three cycles, each of three months duration, and included 881 children from Minamisoma City [Tsubokura et al., 2015]. Similar to other studies, the natural background dose was assumed to be the same for all children and equal to 0.14 mSv for each three-month period of the study (deduced from the annual background dose of 0.54 mSv). The measured anthropogenic effective doses, 0.13–0.15 mSv, were comparable with this assumed background dose.

68. The average effective doses for the three study periods predicted by M2013 and M2020 are compared in figure A-1.IX with the measured doses reported by Tsubokura et al. [Tsubokura et al., 2015]. Both models predict doses comparable with those measured, with M2013 slightly underestimating and M2020 slightly overestimating them, typically by of the order of about ten or up to a few tens of per cent.

Figure A-1.IX. Comparison of the external effective doses from personal dosimetry data for Minamisoma City school children in 2012–2013 [Tsubokura et al., 2015] and the corresponding dose estimates obtained using M2013 [UNSCEAR, 2014] and M2020 models (this UNSCEAR report)



5. Scenario F: Soma City children

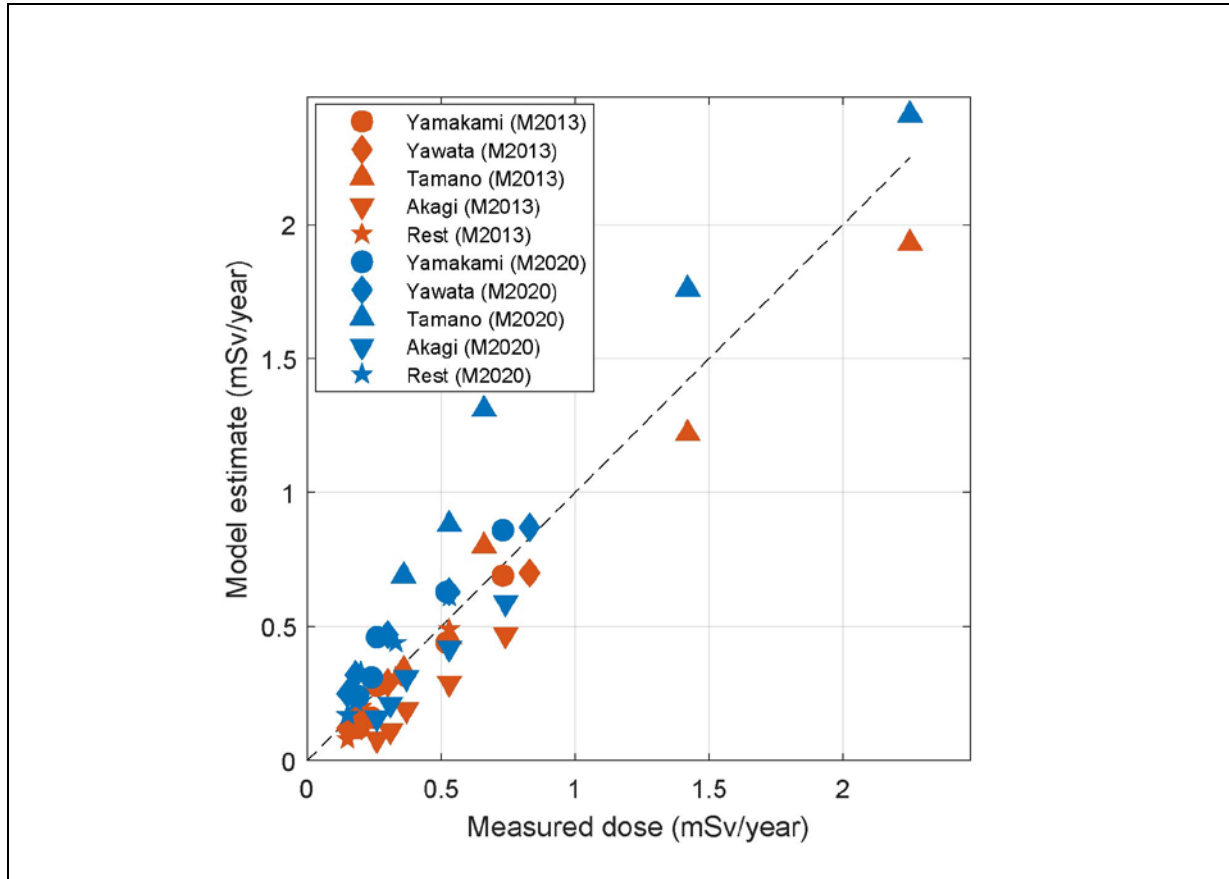
69. The study selected for this validation scenario presented results of the personal dosimetry campaigns conducted in Soma City among preschool and school children from October 2011 to November 2015 [Tsubokura et al., 2017]. The study included five 3-month-long measurement periods in each calendar year: October–December 2011, July–September 2012, May–July 2013, September–November 2014 and September–November 2015.

70. In total, the study involved 14,405 participants among school and preschool children: 3,812 in 2011, 3,824 in 2012, 2,979 in 2013, 1,937 in 2014 and 1,853 in 2015. The children were residents of four areas within Soma City with elevated deposition density (Akagi, Tamano, Yamakami and Yawata) as well as in the rest of the city. The background dose was assumed to be 0.14 mSv for each three-month period of the study, deduced from the annual natural background dose of 0.54 mSv. From 2013 onwards, the reported average anthropogenic doses obtained from the personal dosimeters did not exceed the background dose. Tsubokura et al. [Tsubokura et al., 2017] found that the individual dose distribution was log-normal with a GSD in the range of 1.35–1.75.

71. M2013 and M2020 predicted doses are compared in figure A-1.X with the measurements reported by Tsubokura et al. [Tsubokura et al., 2017]. The data points for each of the five areas within the city are shown for the period 2011–2015 and demonstrate a reduction in dose with time. The model predictions are broadly comparable with the measurements and their reduction over time. M2020 provides a better overall fit to the measured doses with M2013 tending to underestimate them. The spread of the data in figure A-1.X around the diagonal (dashed line)

reflects the uncertainty of the model estimates due to uncertainties in model parameters, in the deposition density levels, and assumptions regarding the people's behaviour and housing; typically the uncertainty can be characterized as not exceeding a factor of two.

Figure A-1.X. Comparison of the external effective doses from personal dosimetry data for Soma City children in 2011–2015 [Tsubokura et al., 2017] and the dose estimates obtained using M2013 [UNSCEAR, 2014] and M2020 models (this UNSCEAR report)



6. Scenario G: Adults in Minamisoma City

72. This scenario was derived from a study [Tsubokura et al., 2018] conducted in Minamisoma City in 2017 among 25 adult indoor workers. The duration of the study was only two weeks and the measured total (anthropogenic plus natural background) doses were used to compare with the similar values obtained in other prefectures distant from Fukushima Prefecture. The measured average total dose was $27 \pm 6 \mu\text{Sv}$ for the two-week period which corresponds to an annual total effective dose of 0.7 mSv. Assuming the annual background dose to fall within the range of 0.54 mSv (typical of Minamisoma City) to 0.63 mSv (typical of Fukushima City), the measured annual anthropogenic dose would be in the range of 0.07 to 0.16 mSv with very large uncertainty. Comparison with model estimates (approximately equal to 0.07 mSv) would not be informative in this case.

C. Outcomes of the personal dosimetry surveys in Minamisoma City and Naraha Town for 2014–2019

73. The municipalities of Minamisoma City and Naraha Town provided the Committee with anonymous data on personal doses measured using luminescence dosimeters. The data included information on the town or municipality of residence, personal age and sex as well as the net measured dose (Minamisoma City) or the total measured dose (Naraha Town). The data provided were grouped in three age ranges, preschool children represented by a 1-year-old infant, school children represented by a 10-year-old child, and adults. No significant differences were found between male and female doses, so sex-averaged doses were used in comparisons with the model estimates.

74. Data for those who wore a dosimeter for 90 days or longer, and whose dosimeters were processed within 80 days after collection, were selected for further analysis. The data set from Minamisoma City contained only net doses for which many were reported blank, presumably, due to being below detection level. The reported data for Naraha Town were total measured doses from which the background dose was subtracted assuming an annual background dose of 0.54 mSv (i.e., the value assumed in other studies in Minamisoma City [Nomura et al., 2015; Nomura et al., 2016; Tsubokura et al., 2015; Tsubokura et al., 2017; Tsubokura et al., 2018]). If the subtraction resulted in a negative value, then this value was replaced by zero in the analysed data set.

75. Dose distributions for the three age groups in each location were analysed. A substantial part of the measured data comprised zero doses. Cumulative distributions for each data set and age group were analysed and empirical percentiles were evaluated for the following cumulative probabilities: 0.25 (if non-zero), 0.5, 0.75, 0.9, 0.95 and 0.975. From these percentiles, assuming log-normality of the distributions, GSD was estimated, which, in combination with the median (assumed GM), was used to compute AM and other statistics, including minimum and maximum values, confidence intervals and the fraction of non-zero measurements. Most of the dose distributions were reasonably close to log-normal, sometimes showing indications of multimodality (Odaka area of Minamisoma City).

76. The data provided by the local authorities of Minamisoma City and Naraha Town enabled direct comparison between the measured and the modelled doses. In the figures A-1.XI–XIII below, both the M2020 (solid line) and M2013 (dashed line) doses are compared with those measured (circle – 50th percentile, star – AM, error bars – 68% confidence interval, the number is the sample size) for three age groups. Based on the information provided by Minamisoma City: (a) 92% of the population was considered to be living in wooden houses and the remaining 8% in brick or concrete buildings; (b) occupancy factors were modified to account for the reported working hours of kindergartens, schools and offices; and (c) all kindergartens were assumed to be in wooden buildings.

1. Haramachi area of Minamisoma City

77. The residents of the Haramachi area in Minamisoma City were the largest group among those measured and, as such, are the best source of drawing statistical inferences from the data. The measured and modelled dose rates, in terms of mSv/year, are shown in figure A-1.XI below, where circles indicate GM, stars – AM, error bars show the 1-sigma ($P = 0.683$) confidence intervals and numbers indicate the number of people measured.

78. M2020 significantly outperforms M2013 and falls within the 68% confidence interval for individual distributions for adults and school children; it does, however, overestimate doses for preschool children by a factor of about two, approaching the upper boundary of the confidence interval. Two factors may have contributed to this difference: firstly, the assumption that all kindergartens were in wooden buildings; and, secondly, the deposition density data used for the modelled doses may not have been representative for the group measured.

79. The modelled and measured doses in the figures demonstrate compatible time dependence of the 3-month-average doses in the studied period.

80. Median values of the measured anthropogenic doses were all small (i.e., lower than the natural background) and are, therefore, themselves associated with significant uncertainty. Substantial variability in the natural background dose between individuals in the studied groups was a likely cause of the reported doses of zero for about 30–50% of preschool children, 17–40% of school children and 18–30% of adults.

2. Kashima area of Minamisoma City

81. Results for a smaller group of residents of the Kashima area in Minamisoma City are shown in figure A-1.XII. The M2020 dose estimates are broadly comparable with those measured and with their variation over time. The agreement is best for the preschool children, with moderate underestimation of doses for school children and adults. The model estimates, however, fall within the 1-sigma ($P = 0.683$) confidence interval. The M2020 doses are in better agreement with the measurements than those from M2013 which systematically underestimates them.

82. The measured data for the Kashima area show zero values for about 14–55% of preschool children, 25–60% of school children and 22–37% of adults.

Figure A-1.XI. Three-month-averaged effective dose rates for population groups in Haramachi area of Minamisoma City measured by personal dosimeters (symbols, error bars) and calculated with M2013 (dashed line) and M2020 (solid line) for: (a) preschool children; (b) school children; and (c) adults. The numbers indicate the sample size for each data point

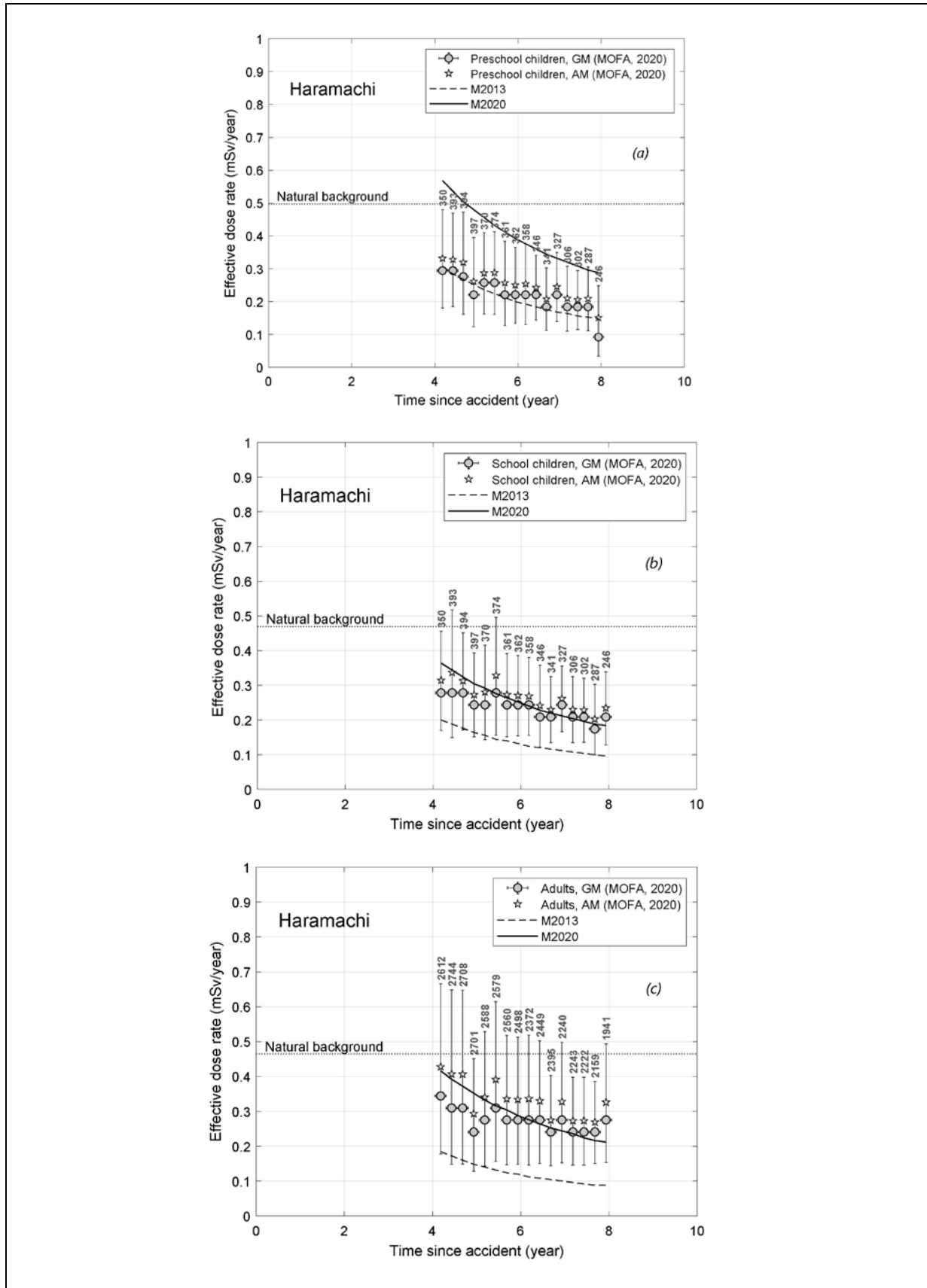
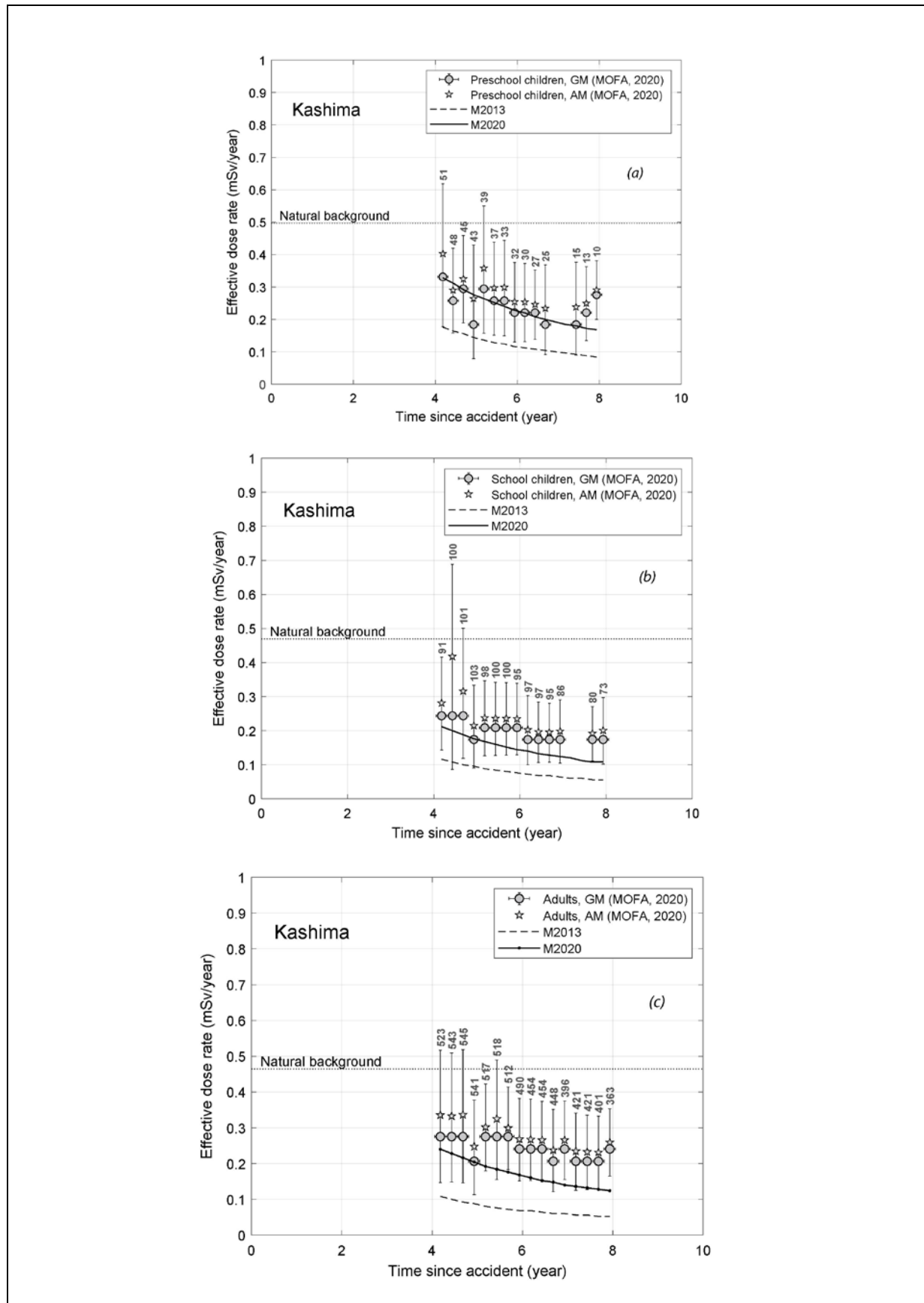


Figure A-1.XII. Three-month-averaged effective dose rates for population groups in Kashima area of Minamisoma City measured by personal dosimeters (symbols, error bars) and calculated with M2013 (dashed line) and M2020 (solid line) for: (a) preschool children; (b) school children; and (c) adults. The numbers indicate the sample size for each data point



3. Odaka area of Minamisoma City

83. Results for an even smaller group of residents of the Odaka area in Minamisoma City are summarized in table A-1.10. The fraction of non-zero doses in the measured groups was often less than 50%, making it impossible to determine median and related statistics of the distribution of doses. For such cases, only the span of the measured doses, bounded by the minimum and the maximum, and 90% confidence intervals are tabulated to enable comparison with the modelled doses. Due to limited sample size and incomplete statistical parameters, the results for the Odaka area are not shown in a figure.

84. Despite the rather low statistical power of these data, M2020 provides a better fit to the measured doses and clearly outperforms M2013, which tends to underestimate them.

Table A-1.10. Statistical properties of the personal dosimetry monitoring data for residents of the Odaka area of Minamisoma City in the period 2015–2019 and comparison with the M2013 and M2020 estimates for a hypothetical matching population

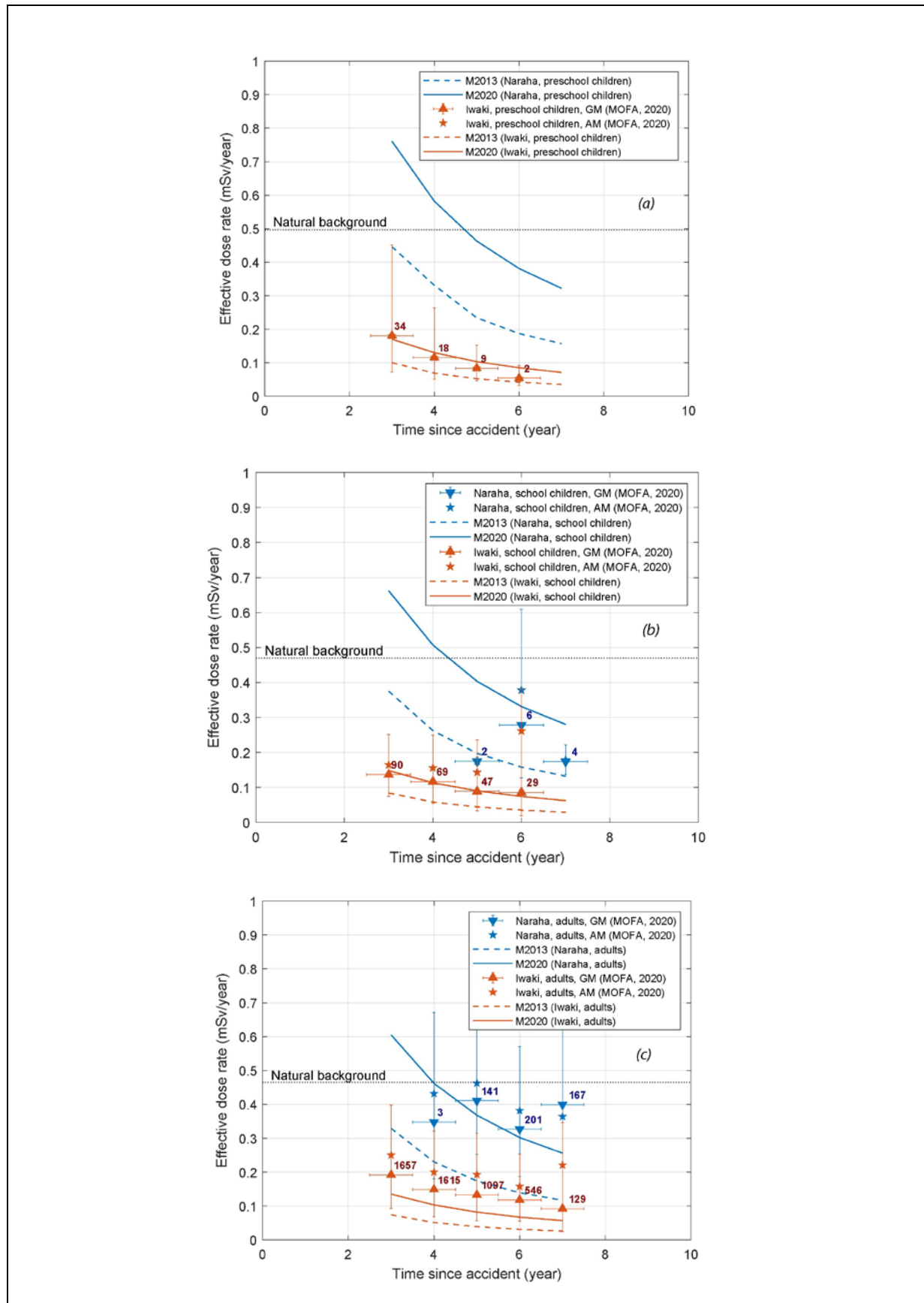
Time	Number of people	Non-zero (%)	Effective dose for 3 months (mSv)									
			Measured							Modelled		
			Min.	Max.	AM	GM	GSD	q(5%)	q(95%)	M2013	M2020	
Preschool children												
2015, Q2	38	32	0	0.18					0	0.13	0.08	0.14
2015, Q3	37	38	0	0.15					0	0.13	0.07	0.13
2015, Q4	34	29	0	0.15					0	0.12	0.07	0.13
2016, Q1	25	32	0	0.11					0	0.11	0.06	0.12
2016, Q2	24	46	0	0.12					0	0.11	0.06	0.11
2016, Q3	26	38	0	0.12					0	0.11	0.06	0.11
2016, Q4	24	46	0	0.11					0	0.11	0.05	0.10
2017, Q1	20	35	0	0.10					0	0.10	0.05	0.10
2017, Q2	17	41	0	0.10					0	0.10	0.05	0.09
2017, Q3	14	43	0	0.12					0	0.12	0.05	0.09
2017, Q4	14	36	0	0.09					0	0.09	0.04	0.09
2018, Q1	12	42	0	0.12					0	0.12	0.04	0.08
2018, Q2	9	56	0	0.11	0.06	0.05	1.8		0	0.11	0.04	0.08
2018, Q3	7	57	0	0.14	0.07	0.06	1.8		0	0.14	0.04	0.08
2018, Q4	9	44	0	0.13					0	0.13	0.04	0.07
2019, Q1	5	60	0	0.13	0.09	0.08	1.3		0	0.13	0.04	0.07
School children												
2015, Q2	70	41	0	0.22					0	0.10	0.05	0.09
2015, Q3	71	39	0	0.22					0	0.13	0.05	0.08
2015, Q4	74	39	0	0.15					0	0.11	0.04	0.08
2016, Q1	78	27	0	0.12					0	0.08	0.04	0.08
2016, Q2	75	27	0	0.13					0	0.09	0.04	0.07
2016, Q3	81	32	0	0.15					0	0.11	0.04	0.07
2016, Q4	74	24	0	0.12					0	0.10	0.03	0.07
2017, Q1	74	27	0	0.12					0	0.10	0.03	0.06

Time	Number of people	Non-zero (%)	Effective dose for 3 months (mSv)								
			Measured							Modelled	
			Min.	Max.	AM	GM	GSD	q(5%)	q(95%)	M2013	M2020
2017, Q2	72	29	0	0.12				0	0.10	0.03	0.06
2017, Q3	66	32	0	0.12				0	0.11	0.03	0.06
2017, Q4	67	33	0	0.13				0	0.10	0.03	0.05
2018, Q1	57	40	0	0.12				0	0.09	0.03	0.05
2018, Q2	46	33	0	0.15				0	0.11	0.03	0.05
2018, Q3	49	35	0	0.13				0	0.10	0.03	0.05
2018, Q4	50	34	0	0.15				0	0.13	0.03	0.05
2019, Q1	37	38	0	0.13				0	0.10	0.02	0.05
Adults											
2015, Q2	726	63	0	1.41	0.09	0.05	2.9	0	0.34	0.05	0.10
2015, Q3	755	63	0	1.16	0.09	0.05	2.8	0	0.34	0.04	0.10
2015, Q4	767	64	0	1.15	0.08	0.05	2.7	0	0.35	0.04	0.09
2016, Q1	752	49	0	0.86				0	0.30	0.04	0.09
2016, Q2	725	64	0	0.90	0.08	0.05	2.4	0	0.26	0.04	0.08
2016, Q3	718	66	0	0.79	0.08	0.05	2.4	0	0.28	0.03	0.08
2016, Q4	718	62	0	0.70	0.07	0.05	2.3	0	0.25	0.03	0.08
2017, Q1	706	61	0	1.31	0.07	0.05	2.3	0	0.24	0.03	0.07
2017, Q2	624	63	0	1.45	0.08	0.05	2.5	0	0.26	0.03	0.07
2017, Q3	645	62	0	0.81	0.08	0.05	2.5	0	0.27	0.03	0.07
2017, Q4	639	57	0	0.79	0.07	0.05	2.2	0	0.24	0.03	0.06
2018, Q1	589	59	0	0.84	0.07	0.05	2.2	0	0.24	0.03	0.06
2018, Q2	579	55	0	1.94	0.07	0.04	2.6	0	0.22	0.02	0.06
2018, Q3	599	56	0	0.52	0.07	0.04	2.6	0	0.22	0.02	0.06
2018, Q4	573	56	0	0.52	0.07	0.05	2.2	0	0.23	0.02	0.05
2019, Q1	533	60	0	0.65	0.07	0.05	2.3	0	0.21	0.02	0.05

4. Naraha Town (Iwaki)

85. Measured doses for residents of Naraha Town, currently living in Naraha or in Iwaki, are compared with model estimates in figure A-1.XIII. The M2020 estimates demonstrate good agreement with the measured data, being somewhat low for the adults from Naraha currently living in Iwaki. The higher measured doses may be a result of deposition density of radiocaesium at their home or place of work differing from those assumed in the model estimates.

Figure A-1.XIII. Three-month-averaged effective dose rates for population groups in Naraha Town (blue) and Iwaki City (orange) measured by personal dosimeters (symbols, error bars) and calculated with M2013 (dashed line) and M2020 (solid line) for: (a) preschool children; (b) school children; and (c) adults. The numbers indicate the sample size for each data point

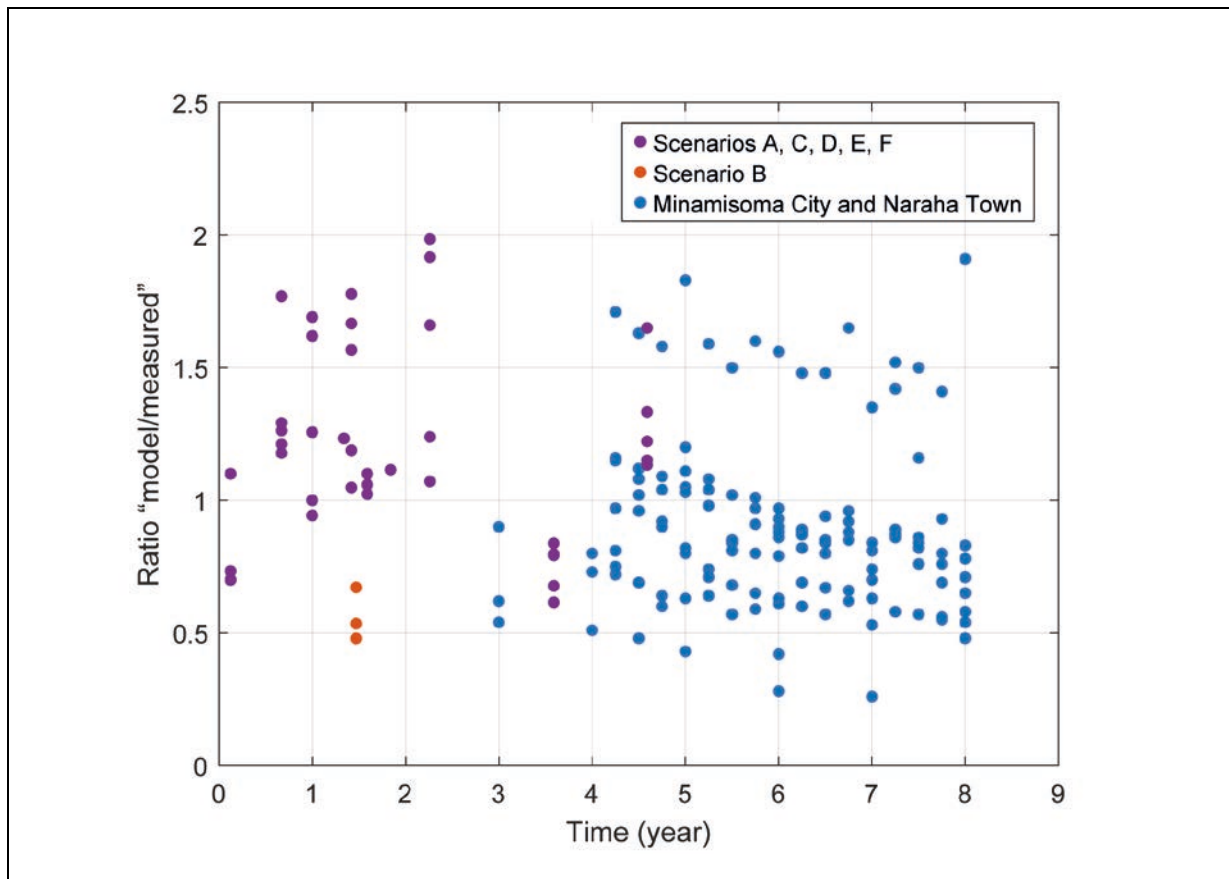


D. Summary

86. Predictions of doses estimated by M2013 and M2020 have been compared with those measured in personal dosimetry campaigns carried out in various areas of Fukushima Prefecture. In most cases, M2020 outperforms M2013 and fits better the measured doses. The only exception is scenario B [Harada et al., 2014] where the estimates of both models are systematically less than the reported measured values.

87. The ratio of M2020 model-calculated external doses and the estimates obtained from the validation scenarios derived from the published results of personal dosimetry studies, as well as based on the external doses measured by personal dosimeters as reported by the authorities of Minamisoma City and Naraha Town is shown in figure A-1.XIV. The plotted ratios span the period from 2011 to 2019 and fall within a range of 0.25 to 2. The mean ratio over the whole period is 0.965 and the 90% confidence interval is from 0.53 to 1.67.

Figure A-1.XIV. Ratio of model-calculated and measured group-averaged values of external doses from the validation scenarios (violet and orange symbols) and data from Minamisoma City and Naraha Town (blue symbols)



88. M2020 was derived using the extensive monitoring data collected after the accident and, due to this, it adequately characterizes the observed dynamics of ambient dose rate over the first decade after the accident in semi-natural and anthropogenic environments of Fukushima Prefecture. Due to the decreasing trend of the ambient dose rate, uncertainty in the long-term component (which describes the dose rate dynamics decades into the future), would not contribute significantly to the time integral of dose.

89. Most of the measured doses were small and close to the assumed background levels. This results in additional uncertainty or bias if the real background values were higher than assumed.

The results reported by Nomura et al. [Nomura et al., 2019] for the study in Fukushima Prefecture showed that, after subtraction of the background dose, the measured anthropogenic doses were zero for: 62.5% of the measured population outside Minamisoma City; 33% of the residents of Haramachi and Kashima areas; and 10.5% of those returned to the previously evacuated Odaka area. These results clearly indicate that the unknown spatial and temporal variability in the natural background radiation challenges accurate determination of relatively small anthropogenic doses. Future studies are needed to better characterize variability of the background doses and to quantify the uncertainties in those measured.

E. Variability of individual external doses in Fukushima Prefecture

90. Along with the uncertainty of the external doses for certain groups of residents of municipalities in Fukushima Prefecture, described in section III.I, it is of interest to estimate variability among individuals around the average values. Within one municipality, an individual dose may depend on non-uniform distribution of radionuclides across its territory, site development, the type of residential building, occupancy, lifestyle and household habits, etc.

91. The Committee evaluated the variability in individual doses by statistical processing of individual monitoring data from several municipalities. Databases of large-scale monitoring programmes, conducted by the municipal authorities of Minamisoma City (2015–2019, 64,996 measurements, 3,400–4,900 per quarter), Iwaki City and Naraha Town (2014–2018, 7,062 measurements), were provided by the municipality authorities [Minamisoma, 2019] and were analysed. For each data set for a monitoring period from one to three months, statistical characteristics were calculated for three population groups (adults, school children, and preschool children) in each municipality. Published data on statistical properties of individual dose distributions obtained from personal dosimetry studies were also used, including 499 measurements among adults of Fukushima City in 2012 [Takahara et al., 2014] and 520 measurements of school children in Minamisoma City in 2012 [Nomura et al., 2016]. These characteristics of the distributions normalized to the corresponding average dose and averaged for all studies are shown in table A-1.11.

Table A-1.11. Variability of measured individual external doses in Fukushima Prefecture (ratio of percentiles to average values, unitless)

<i>Population group</i>	<i>Parameters of effective dose distributions (relative units)</i>			
	<i>5%</i>	<i>50%</i>	<i>Average</i>	<i>95%</i>
Preschool children	0.38	0.88	1.00	2.03
School children	0.35	0.86	1.00	2.12
Adults	0.28	0.81	1.00	2.37

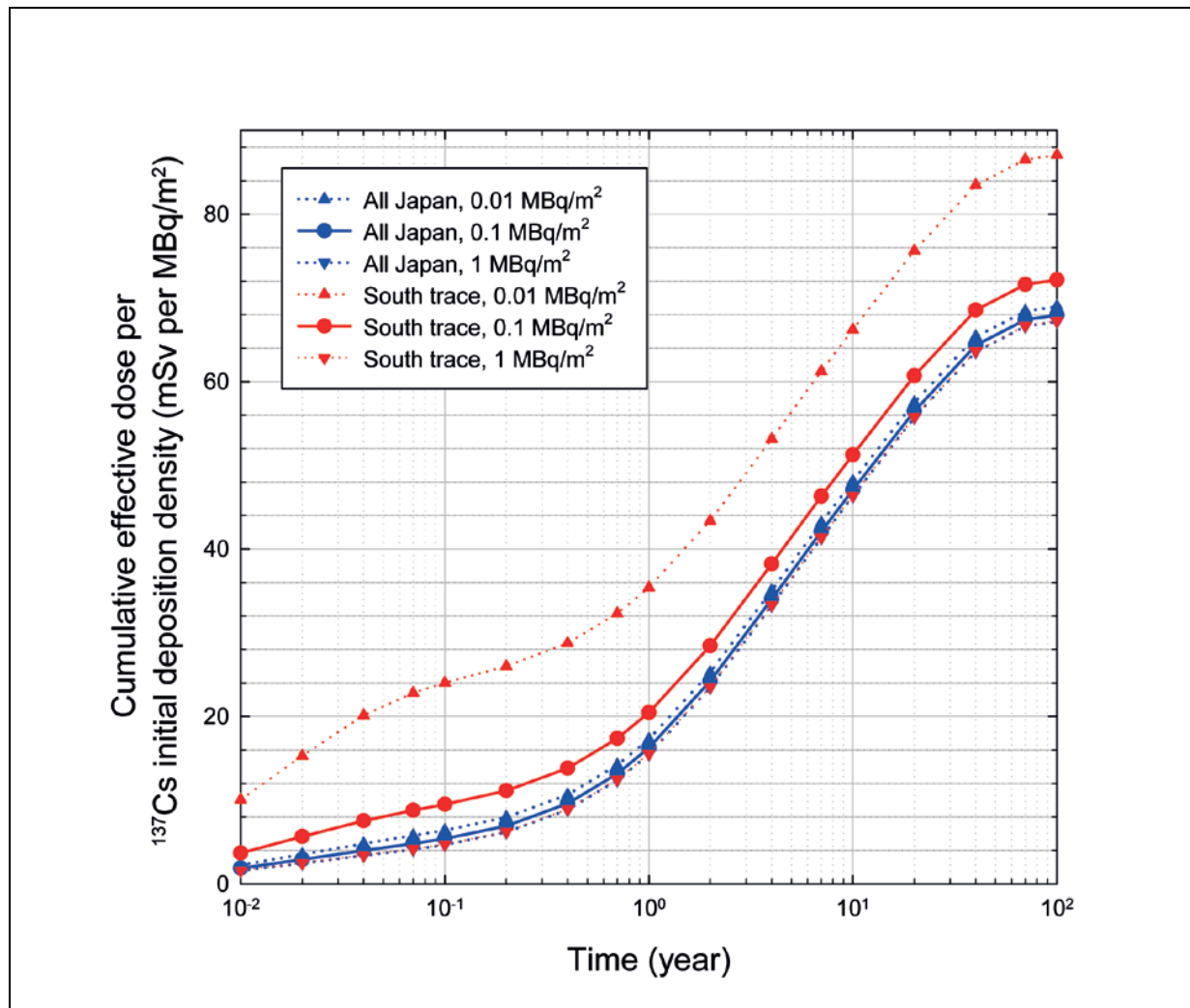
92. Statistical parameters presented in table A-1.11 demonstrate moderate variability of individual external doses. The measured external doses for 5% of the monitored persons do not exceed the value which is by 2.6–3.6 times less than the average dose and the 5% received highest doses which exceed the average value by a factor of 2 to 2.4. The dose variability is slightly more in adults than in children presumably because of greater variability in their occupancy (e.g., outdoor and indoor workers, etc.). The Committee has judged that the variability parameters summarized in table A-1.11, can be considered applicable to the whole of Fukushima Prefecture and for other exposure periods.

V. RESULTS OF THE MODEL CALCULATIONS

A. Cumulative doses of external exposure per unit ^{137}Cs deposition density

93. M2020 differs from M2013 [UNSCEAR, 2014] in several respects, including non-linear approximations for initial radionuclide activity concentration ratios in deposited material. The latter results in different time integrals of external dose per unit initial deposition density of ^{137}Cs , depending on different contributions to the dose from shorter-lived radionuclides and whether the deposition is in the South trace or elsewhere and on the ^{137}Cs deposition density. Similar to that shown in [UNSCEAR, 2014], figure A-1.XV presents the time dependence of the cumulative effective dose per unit deposition density of ^{137}Cs for areas located in the South trace and the rest of the country and for three different values of the ^{137}Cs deposition density: 10 and 100 kBq/m² and 1 MBq/m². The calculated doses are for an adult living in a wooden house and working indoors in a concrete building (assumed to be representative of a typical adult).

Figure A-1.XV. Accumulation of effective dose from external exposure per unit ^{137}Cs deposition density with time after the accident for areas with different initial ^{137}Cs deposition density on the territories of the South trace (red symbols and lines) and the rest of Japan (blue symbols and lines). The cumulative effective doses are shown for the initial deposition densities of ^{137}Cs : 0.01 (upward triangles, dashed lines), 0.1 (circle, solid lines) and 1 (downward triangles, dashed lines) MBq/m²



94. For ^{137}Cs deposition density 100 kBq/m^2 , M2020 predicts cumulative effective doses higher than those estimated using M2013 [UNSCEAR, 2014] by 18% for the South trace and about 50% for the rest of Japan.

95. Unlike M2013, the cumulative effective dose in M2020 per unit initial deposition density of ^{137}Cs depends on the latter due to use of non-linear approximations (see equation A-1.3 and table A-1.2) for radionuclide activity concentration ratios. Correspondingly, for lower ^{137}Cs deposition density the cumulative effective dose per unit ^{137}Cs deposition density increases, especially for the South trace (see dashed curves and upward pointing triangles in figure A-1.XV for 10 kBq/m^2 of ^{137}Cs); the relative contribution of shorter-lived radionuclides is greater for the areas with lower radionuclide deposition densities. On the other hand, due to use of non-linear approximations the difference between cumulative doses for areas in the South trace and in the rest of Japan decreases when deposition density ^{137}Cs increases and at ^{137}Cs deposition density of 1 MBq/m^2 becomes almost indistinguishable (see dashed curves and downward pointing triangles in figure A-1.XV).

96. Cumulative effective doses, estimated using M2020 and M2013 for initial ^{137}Cs deposition density 100 kBq/m^2 , are compared in table A-1.12 for representatives of various age and social groups for the period 1 year, and 10 years after the accident, as well as for the period up to age 80, for preschool children, school children and adult workers at the time of the accident. The selected value of 100 kBq/m^2 for ^{137}Cs initial deposition density is representative of non-evacuated areas in Japan with higher deposition densities of radiocaesium.

Table A-1.12. Cumulative effective dose (mSv) from external exposure, estimated for initial deposition density 100 kBq/m^2 of ^{137}Cs as of June 2011, for various members of the public from time of the accident onwards

Exposure duration	Cumulative effective dose (mSv) for members of the public as of 2011 for initial ^{137}Cs deposition density 100 kBq/m^2 in June 2011							
	1-year-old (preschool children)		10-year-old (school children)		Adult outdoor worker		Adult indoor worker	
	M2013	M2020	M2013	M2020	M2013	M2020	M2013	M2020
Entire Japan except the South trace ^a								
1 year	2.1	2.3	1.8	1.9	1.8	2.6	1.6	1.6
10 years	4.9	6.3	4.2	5.4	3.9	7.6	3.8	4.7
Lifetime ^b	6.7	8.5	6.0	7.6	5.6	10.8	5.6	6.7
The South trace ^a								
1 year	4.9	2.9	4.1	2.4	4.0	3.2	3.7	2.0
10 years	7.6	6.9	6.5	5.9	6.2	8.2	5.9	5.1
Lifetime ^b	9.4	9.1	8.3	8.1	7.9	11.5	7.7	7.1

^aThe municipalities of Naraha, Hirono, Yamatsuri and Iwaki City of Fukushima Prefecture, and the towns of Kitaibaraki and Takahagi of Ibaraki Prefecture.

^bTime up to age 80, assuming 20-year-old adult at the time of the accident.

B. Doses from external exposure in the first year following the Fukushima Daiichi Nuclear Power Station accident

97. Doses from external exposure in the first year following the accident have been estimated for non-evacuated municipalities of Fukushima Prefecture (Group 2), for some neighbouring prefectures (Group 3) and for all other prefectures in the rest of Japan (Group 4). Prefecture-average doses for Groups 2, 3 and 4 prefectures are shown in table A-1.13. For Group 3 prefectures and for Fukushima Prefecture, the ranges of municipality-averaged doses are given. For Chiba, Gunma and Iwate (close to Fukushima Prefecture and with enhanced deposition densities in comparison to other Group 4 prefectures) the prefecture-average doses are tabulated. For the remaining Group 4 prefectures, the range of prefecture-averaged values is indicated.

Table A-1.13. Estimated municipality- or prefecture-average effective doses from external exposure in the first year following the accident for those residing in the areas indicated

<i>Municipality or prefecture</i>	<i>The first-year effective dose (mSv)</i>		
	<i>Adult</i>	<i>10-year-old</i>	<i>1-year-old</i>
Group 2 – Fukushima Prefecture ^a			
Municipalities not evacuated ^b	0.04–3.6	0.05–4.2	0.06–5.0
Group 3 – the neighbouring prefectures ^c			
Ibaraki Prefecture	0.13–0.73	0.16–0.87	0.19–1.03
Miyagi Prefecture	0.09–0.85	0.11–1.01	0.13–1.20
Tochigi Prefecture	0.28–0.90	0.33–1.07	0.39–1.26
Yamagata Prefecture	0.08–0.11	0.09–0.13	0.11–0.15
Group 4 – the rest of Japan ^d			
Chiba Prefecture	0.35	0.42	0.50
Gunma Prefecture	0.23	0.28	0.33
Iwate Prefecture	0.20	0.24	0.29
39 remaining prefectures	0.00–0.15	0.0–0.18	0.0–0.21

^a Group 2: members of the public living in the non-evacuated municipalities of Fukushima Prefecture.

^b Excluding evacuated areas within Fukushima Prefecture.

^c Group 3: members of the public living in the prefectures of Ibaraki, Miyagi, Tochigi and Yamagata.

^d Group 4: members of the public living in Chiba, Gunma and Iwate prefectures and the remaining 39 prefectures.

98. The doses in table A-1.13 are average values within a designated municipality or prefecture; where ranges of dose are indicated these are the ranges of average values between different municipalities within one or other prefecture, or between prefectures within a given Group. They do not represent the variability in individual doses within one or other municipality or prefecture.

99. M2020 takes into account age- and social group-specific occupancy factors and different shielding properties of the typical houses in Japan. Ratios of the average first-year dose for the four main population groups considered (see table A-1.8) to that for a “typical adult”, assumed to be an adult indoor worker living in a wooden one-to-three storey house, are shown in table A-1.14. The variation in the average first-year dose between the groups ranges from 0.5–1.6.

Table A-1.14. Ratios of the effective dose from external exposure in the first year to each of the various age/population groups of the Japanese population to that of an adult living in a wooden house and working indoors in a concrete building

<i>Dwelling type</i>	<i>Ratio of the first-year effective doses (dimensionless)</i>			
	<i>Adult worker</i>		<i>10-year-old</i>	<i>1-year-old</i>
	<i>Indoor</i>	<i>Outdoor</i>		
Wooden, one-to-three-storey house	1.0	1.6	1.2	1.4
Wooden fireproof, one-to-three-storey house	0.7	1.2	0.8	0.9
Concrete, multi-storey apartment	0.5	1.0	0.6	0.7

C. Cumulative doses from external exposure for the population of Japan

100. The cumulative doses of external exposure for different groups of the population of Japan were calculated for various areas of the whole country. Conditional on degree of detail of the available data on deposition density of radionuclides and on the value of anticipated dose, the calculated data represent various spatial scales, ranging from municipality-averaged doses in Fukushima Prefecture and some proximal prefectures (Groups 2 and 3) to prefecture-averaged values for the territories in the rest of the country (Group 4). The ranges of the computed values for the Group 2, 3 and 4 territories are shown in table A-1.15.

Table A-1.15. Estimated municipality- or prefecture-averaged effective doses from external exposure for adults, 10-year-old children and 1-year-old infants at the time of the accident over the first year and the first 10 years and to age 80 years

<i>Age group in March 2011</i>	<i>Municipality- or prefecture-averaged effective dose^a (mSv)</i>		
	<i>Group 2 Fukushima Prefecture^b</i>	<i>Group 3 Neighbouring prefectures^c</i>	<i>Group 4 The rest of Japan^d</i>
1-year exposure			
Adult	0.04–3.6	0.09–0.74	0.0–0.35
10-year-old	0.05–4.2	0.10–0.88	0.0–0.42
1-year-old	0.06–5.0	0.12–1.0	0.0–0.50
10-year exposure			
Adult	0.12–10.6	0.22–2.1	0.0–1.0
10-year-old	0.13–12.0	0.25–2.3	0.0–1.1
1-year-old	0.16–14.1	0.29–2.7	0.0–1.3
Lifetime exposure to age 80 years			
Adult ^e	0.17–15.1	0.30–2.9	0.0–1.4
10-year-old	0.18–16.7	0.34–3.2	0.0–1.6
1-year-old	0.21–19.0	0.38–3.7	0.0–1.78

^a The reported doses are ranges of municipality-average doses for the Group 2 and Group 3 prefectures and ranges of prefecture-average doses for the Group 4 prefectures. The ranges of dose tabulated reflect the variation in average doses between different municipalities within one or other prefecture, or between prefectures within a given Group; they do not reflect the variability of doses received by individuals within one or other designated municipality or prefecture.

^b Non-evacuated municipalities of Fukushima Prefecture.

^c The prefectures of Ibaraki, Miyagi, Tochigi and Yamagata.

^d The prefectures of Chiba, Gunma and Iwate and the remaining 39 prefectures.

^e Assumed to be a 20-year old.

D. Post-remediation doses

101. Since 2013, extensive remediation work has been underway in the regions of Japan with the higher deposition densities to reduce the dose rate and concentrations of radionuclides in areas from which people were evacuated (special decontamination area (SDA)) or continue to live and grow food (intensive contamination survey area (ICSA)). This work includes the use of technologies for decontamination of inhabited areas, and of countermeasures in agriculture (such as top soil removal or reverse tillage or ploughing, additional fertilization, etc.) and in forestry (such as the removal of fallen leaves and other plant material). The experimental studies and tests in Fukushima Prefecture were basically completed in 2012. A large-scale environmental remediation programme was then launched in the affected areas of Fukushima Prefecture and some neighbouring prefectures.

102. In some ICSA areas, local authorities initiated early remediation activities focused mostly on public areas and, especially, in children's and public facilities (kindergartens, schools, hospitals and so on). Similar work, although in the temperate European environment, was intensively conducted in the Chernobyl-affected areas three decades ago, and the conclusions and recommendations from this work were summarized by the Chernobyl Forum [IAEA, 2006] and UNSCEAR [UNSCEAR, 2011].

103. The most intensive remediation in Japan was conducted in 2013–2017, in 11 SDA municipalities of Fukushima Prefecture. This work included implementation of various tested clean-up technologies in public facilities, residential areas, farmland, forest areas and roads [IAEA, 2015a]. Remediation of the SDA was completed at the end of March 2017. Post-remediation monitoring, implemented six months to a year after the remediation work was completed, demonstrated a further reduction in dose rates in all remediated environments.

104. The effectiveness of remediation when assessing public doses is normally quantified using the dose reduction factor (DRF)⁴ which subtracts the effects of radioactive decay and migration of radionuclides in the soil [Balonov et al., 1992; IAEA, 2006; IAEA, 2015c; Ulanovsky et al., 2011]. The Japanese Ministry of the Environment (MOE) made an estimate of the external dose reduction in 2015 [MOE, 2020a], based on the results of 330,000 air dose rate measurements taken before and after remediation and conducted in five types of areas⁵ (public facilities, residential areas, roads, farmland and forests), between March 2012 and October 2013, in 10 SDA municipalities in Fukushima Prefecture and 90 ICSA municipalities in 8 prefectures. To estimate the annual dose for residents and, separately, for schoolchildren, a simple model was applied which multiplied the dose rate by the duration of a person's stay in each relevant location. The effects of decay of radionuclides and their migration were subtracted from the total decrease in the dose for the period under consideration (August 2011 to August 2013); the model used for the analysis was not described and the parameters of migration were not reported. The results of the MOE model assessment of the efficiency of remediation are shown in table A-1.16 [MOE, 2020a].

105. According to MOE, the effectiveness of large-scale remediation was to reduce the dose from external exposure by about 27% for residents of the SDA and somewhat less, about 22%, for residents of the ICSA. The effectiveness of remediation was similar for children. The percentage reductions shown in table A-1.16 correspond to DRFs of about 1.4 for the SDA and 1.3 for the ICSA.

⁴ DRF is the ratio of dose before remediation to dose after remediation assessed with account for radioactive decay and radionuclide migration.

⁵ No measurements conducted in dwelling houses.

Table A-1.16. Average reduction (in %) of effective dose from external exposure from the accident at the Fukushima Daiichi Nuclear Power Station to residents of remediated municipalities over two years (August 2011–August 2013) [MOE, 2020a]

<i>Population</i>	<i>Area</i>	<i>Total dose reduction (%)</i>	<i>Contribution of natural processes (%)</i>	<i>Contribution of remediation (%)</i>
General public	SDA	67	40	27
	ICSA	62		22
Schoolchildren	SDA	66	40	26
	ICSA	64		24

106. Tsubokura et al. [Tsubokura et al., 2019] assessed the effectiveness of remediation at a site in the ICSA (Minamisoma City) based on measurements of individual external dose on residents. In the earliest period (2013–2014), the reduction in the annual dose in areas that had been remediated was greater than that in areas that had not been remediated by 18% in adults and 14% in children.⁶ In the following year (2014–2015), this difference was 9% in adults and 10% in children, and in 2015–2016, no reliable difference was found. In the same municipality, Minamisoma City, Murakami et al. [Murakami et al., 2019] estimated the reduction in annual dose due to remediation to be 11%, based on individual dose measurements. These measurements on people suggest slightly lower DRFs of 1.1–1.2 in the ICSA.

107. Based on the MOE model calculations [MOE, 2020a; MOE, 2020b] and the partial validation of these calculations by measurements of individual external dose [Murakami et al., 2019; Tsubokura et al., 2019], the Committee has judged that remediation has resulted in a dose reduction factor of about 1.3 in the SDA and of about 1.1 to 1.2 (depending on initial dose rate and decontamination timing) in the ICSA. While these dose reduction factors can be used to provide an indication of the benefits of the remediation work, more reliable estimates of the doses to the public taking account of remediation require much more extensive information from post-remediation measurements of individual doses on people. The results of such post-remediation monitoring have not yet been published or provided to the Committee.

108. The dose reduction factors are in broad agreement with remediation carried out in 1989 in the Bryansk region, an area with some of the highest levels of radionuclide deposition following the Chernobyl accident, where a DRF of around 1.3 was estimated [Balonov et al., 1992]. Ulanovsky et al. [Ulanovsky et al., 2011] estimated a DRF of 1.5 for rural areas of Belarus, the Russian Federation and Ukraine affected by the Chernobyl accident.

109. The completion of the extensive remediation work has enabled the earlier lifting of evacuation orders and the gradual return of people. The return of people has not yet been permitted to the “Areas where Returning is Difficult” in six municipalities (entire Futaba and Okuma Towns and parts of Namie and Tomioka Towns, Iitate and Katsurao Villages). In these six municipalities, further remediation is continuing with the aim of lifting the remaining evacuation orders within the following four to five years.

110. The Committee’s estimates of the external doses that were or would be received in 2019–2021 and up to the age of 80 years by those who were evacuated if they returned to their homes and regular lifestyles are shown in tables A-1.17 and A-1.18 for adults and for 1-year-old infants at the time of evacuation in 2011, respectively. They are based on M2020 and a DRF of 1.3 for the SDA to take account of remediation.

⁶ Samples with less than 40 measurements were excluded.

Table A-1.17. Annual and lifetime effective doses from external exposure of adults (indoor workers) who were evacuated from municipalities in Fukushima Prefecture if they returned to their homes

<i>Municipality</i>	<i>Effective external dose (mSv) in the period</i>			
	<i>2019</i>	<i>2020</i>	<i>2021</i>	<i>Lifetime^a</i>
Futaba Town	2.6	2.4	2.1	38
Hirono Town	0.090	0.080	0.080	1.3
Iitate Village	0.94	0.83	0.75	13
Katsurao Village	0.58	0.52	0.46	7.7
Kawamata Town	0.12	0.11	0.090	1.7
Kawauchi Village	0.12	0.10	0.090	1.5
Minamisoma City (Odaka)	0.15	0.13	0.12	2.0
Namie Town	1.2	1.1	0.95	16
Naraha Town	0.15	0.14	0.12	2.2
Okuma Town	2.3	2.1	1.9	32
Tamura City	0.050	0.040	0.04	0.69
Tomioka Town	1.2	1.1	0.99	18

^a The period for adults aged 20 at the time of the accident from their return in 2019 to age 80.

Table A-1.18. Annual and lifetime effective doses from external exposure of 1-year-old infants at the time of the accident who were evacuated from municipalities in Fukushima Prefecture if they returned to their homes

<i>Municipality</i>	<i>Effective external dose (mSv) in the period</i>			
	<i>2019</i>	<i>2020</i>	<i>2021</i>	<i>Lifetime^a</i>
Futaba Town	3.3	2.9	2.6	40
Hirono Town	0.12	0.10	0.090	1.4
Iitate Village	1.2	1.0	0.93	14
Katsurao Village	0.72	0.64	0.57	8.5
Kawamata Town	0.15	0.13	0.12	1.8
Kawauchi Village	0.14	0.12	0.11	1.8
Minamisoma City (Odaka)	0.18	0.16	0.15	2.2
Namie Town	1.5	1.3	1.2	18
Naraha Town	0.19	0.17	0.15	2.4
Okuma Town	2.9	2.5	2.3	35
Tamura City	0.050	0.050	0.050	0.69
Tomioka Town	1.5	1.4	1.2	19

^a The period for 1-year-old infants at the time of the accident from their return in 2019 to age 80.

111. The external doses calculated for adults using M2020 in table A-1.17 have been compared with recent individual measurements of 239 adults, mostly office workers, living in 10 former evacuated locations, which are listed in table A-1.17, excluding Okuma and Futaba towns [Nomura et al., 2020]. Measurements of external doses were made with personal dosimeters worn by the study participants during 14 days in February 2019. The area-averaged

measured values correspond to annual dose in 10 locations of 0.93 mSv, including dose from background radiation assessed to be 0.54 mSv per year for Fukushima Prefecture. The variability in the estimated mean annual doses in different locations was small, ranging from 0.7–1.1 mSv. Deduction of background dose results in a measured area-averaged anthropogenic annual dose due to residual deposited caesium radionuclides of 0.39 mSv. The M2020 model estimate (see table A-1.17, excluding Okuma and Futaba Towns) including a DRF of 1.3 was 0.46 mSv, which is in good agreement with the measured data [Nomura et al., 2020].

112. In their earlier paper, Nomura et al. [Nomura et al., 2019] estimated, inter alia, annual external doses to 112 people who returned to Odaka Ward (in the SDA) of Minamisoma City following completion of remediation. The median annual dose to a mixed age group of returnees in 2017 was estimated as 0.4 mSv from the three-month individual dose measurements. The Committee's assessed annual dose in 2017 for indoor workers residing in Odaka Ward using M2020 is 0.20 mSv for indoor workers including a DRF of 1.3. However, the estimates of Nomura et al. are for group members who spent more time outdoors than the nominal time assumed for indoor workers in M2020. With the relevant correction, the modelled annual dose in 2017 becomes about 0.25 mSv, which is in reasonable agreement with the individual dose estimated by Nomura et al. from measurements.

VI. SUMMARY

113. The follow-up study of population exposures in Japan after the FDNPS accident was supported by the review and revision of the dose assessment methodology for external exposures to deposited radioactive materials in human habitats and in the environment. Results of the critical review of the new findings and data acquired in Japan after the accident suggested some modifications of the external dose assessment methodology were needed and the careful analysis undertaken has resulted in formulation of the modified model, termed M2020, for calculation of the population doses due to external exposure from radionuclides deposited on the ground. The definition of parameters of M2020 has been based on a comprehensive set of data obtained from extensive and systematic monitoring of affected areas of Japan. M2020 is, therefore, tailored to Japan-specific environmental and social conditions and the post-accidental reality. It inherits many of the features of the model used in the UNSCEAR 2013 Report, M2013, that was largely based on data from global fallout and experience following the accident at the Chernobyl Nuclear Power Station; but, in addition, it has benefited from new observations specific to Japan.

114. M2020 also benefits from the new age- and sex-dependent dose rate coefficients for external environmental radiation sources. Although the changes due to introduction of the new dose rate coefficients are not large, nor do they compromise the dose estimates in the UNSCEAR 2013 Report, they provide the most up-to-date values currently available. Their use enables organ-specific dose estimates for both sexes and explicitly demonstrates the small range of variability associated to mean sex- and organ-specific dose rate coefficients for external exposure to environmental sources.

115. One of the most important changes in M2020 is related to the observed dynamics of the reduction in external dose rate with time due to radioactive decay and various natural processes, of which migration in soil is the most influential. The slower dose rate reduction observed within 5–6 years following the accident was not anticipated based on experience elsewhere and the processes contributing to this slower decrease in dose have yet to be fully understood. Further studies of the physical and chemical properties of the deposited radioactive material, its composition and environmental behaviour may provide necessary information to explain these observations.

116. The environmental conditions in the affected areas of Japan differ substantially from the previously studied areas in Europe and North America, due to presence of mountainous areas, high anthropogenic use of available flatlands and relatively high population density in Japan. It is likely that these differences have contributed to the differences observed relative to experience elsewhere, which required to reconsider the location factors and their dynamics and to use the new approximations to reproduce as observations of ambient dose rate dynamics results of the personal dosimetry studies among the population of Fukushima Prefecture.

117. It was already noticed [IAEA, 2015b; UNSCEAR, 2014] that radionuclide composition of the deposited radioactive material varied considerably across Fukushima Prefecture and in other parts of Japan. M2020 introduces new phenomenologically-based non-linear approximations that better address ratios of deposition densities of radionuclides ^{131}I , ^{132}I , $^{129\text{m}}\text{Te}$ and ^{132}Te to that of ^{137}Cs , which were obtained from the environmental measurements, including recently updated values for ^{131}I based on measurements of the longer-living anthropogenic iodine isotope ^{129}I . Use of the new non-linear approximations enabled account to be taken of systematic differences of radionuclide composition of deposited material between locations with high and low deposition density of ^{137}Cs (see figure A-1.XV).

118. M2020 was validated using: independent results from the FHMS; a number of personal dosimetry studies reported in the peer-reviewed literature; and monitoring data provided by the municipalities of Minamisoma City and Naraha Town. The M2020 predictions were within a factor of about two of the measured doses and provided a better fit to the measurements than M2013, the model used in the UNSCEAR 2013 Report (see figure A-1.XV).

119. Population-weighted average external doses from deposited radioactive material have been calculated using M2020 for the following reference age/social groups of the public (as of 2011) permanently residing in a prefecture or municipality: 1-year-old infants, 10-year-old children, 20-year-old adults (indoor workers) living in wooden houses. For people living in other type of houses (wooden fireproof or concrete multi-storey apartments), ratios of the effective dose from external exposure in the first year for each of the various age/social groups of the Japanese population to that of an indoor worker living in a wooden house have been provided. Both average effective and organ absorbed doses to the three age/social groups of the public were assessed for the following time periods: 1 year and 10 years after the accident, and up to age 80. Additionally, area-averaged in-utero doses to red bone marrow of children born in March–December 2011 and fetal thyroid doses of children born in March–October 2011 in Fukushima Prefecture (excluding evacuated areas) were calculated. Both average effective and organ absorbed doses from external exposure to deposited radionuclides were assessed for evacuees up to the end of the first year after the accident. Average annual effective doses to the three age/social groups of the public in 2021 were also estimated. Collective effective and organ absorbed doses from external exposure received by population of Japan over 1, 10 and 80 years were assessed. External dose estimates are tabulated in attachments A-13 to A-20. In these estimates, no account has been taken of the effects of remediation; the available information indicates that, as a result, doses may have been overestimated by at most 10–20%, which is small compared with the inherent uncertainties in the dose assessment.

120. Estimates have been made of the uncertainty in external doses predicted using M2020 taking account of uncertainties in the input data and model parameters. The 90% confidence interval, averaged over locations and population groups and expressed in terms of the respective AM, was 0.54–1.67 for exposures during the first decade and 0.49–1.76 for lifetime exposures. Given the magnitude of these uncertainties, the small differences observed between measured and modelled doses have little statistical significance.

121. Analysis of anonymous personal dosimetry data provided by the municipalities of Minamisoma City and Naraha Town enabled individual dose distributions to be derived. For the majority of the data sets, the individual doses were log-normally distributed, mostly left-censored and sometimes showing signs of multimodality (e.g., when individual doses for 5–10% of those in the studied group were higher than could be inferred from properties of distribution for the rest of the group). Under the assumption of log-normality, the estimated statistical parameters corresponding to normalized 90% confidence intervals range from 0.3–0.4 to 2–2.4, expressing the degree of individual variability of the measured external doses.

122. Estimates have also been made of external doses from deposited radioactive material for evacuees were they to return to their homes. These were based on M2020 with a dose reduction factor to take account of remediation of 1.3.

REFERENCES

- Akahane, K., S. Yonai, S. Fukuda et al. NIRS external dose estimation system for Fukushima residents after the Fukushima Dai-ichi NPP accident. *Sci Rep* 3: 1670 (2013).
- Andoh, M., S. Mikami, S. Tsuda et al. Decreasing trend of ambient dose equivalent rates over a wide area in eastern Japan until 2016 evaluated by car-borne surveys using KURAMA systems. *J Environ Radioact* 192: 385-398 (2018a).
- Andoh, M., H. Yamamoto, T. Kanno et al. Measurement of ambient dose equivalent rates by walk survey around Fukushima Dai-ichi Nuclear Power Plant using KURAMA-II until 2016. *J Environ Radioact* 190-191: 111-121 (2018b).
- Balonov, M.I., V.Y. Golikov, V.G. Erkin et al. Theory and practice of a large-scale programme for the decontamination of the settlements affected by the Chernobyl accident. *Radiation Protection-54*, Report EUR 14469. 1992.
- Eged, K., Z. Kis and G. Voigt. Review of dynamical models for external dose calculations based on Monte Carlo simulations in urbanised areas. *J Environ Radioact* 85(2-3): 330-343 (2006).
- Golikov, V.Y., M.I. Balonov and P. Jacob. External exposure of the population living in areas of Russia contaminated due to the Chernobyl accident. *Radiat Environ Biophys* 41(3): 185-193 (2002).
- Harada, K.H., T. Niisoe, M. Imanaka et al. Radiation dose rates now and in the future for residents neighboring restricted areas of the Fukushima Daiichi Nuclear Power Plant. *Proc Natl Acad Sci U S A* 111(10): E914-923 (2014).
- IAEA. Environmental consequences of the Chernobyl accident and their remediation: Twenty years of experience. Report of the Chernobyl Forum Expert Group "Environment". International Atomic Energy Agency, Vienna, 2006.
- IAEA. The Fukushima Daiichi accident. Technical volume 5. Post-accident recovery. International Atomic Energy Agency, Vienna, 2015a.
- IAEA. The Fukushima Daiichi accident. Technical volume 1. Description and context of the accident. International Atomic Energy Agency, Vienna, 2015b.
- IAEA. The Fukushima Daiichi accident. Report by the Director General. International Atomic Energy Agency. Vienna, 2015c.
- IAEA. The Fukushima Daiichi accident. Technical volume 4. Radiological consequences. International Atomic Energy Agency, Vienna, 2015d.
- ICRP. Report on the task group on reference man. ICRP Publication 23. International Commission on Radiological Protection, Pergamon Press, Oxford, 1975.
- ICRP. Conversion coefficients for use in radiological protection against external radiation. ICRP Publication 74. *Annals of the ICRP* 26(3-4). International Commission on Radiological Protection, Pergamon Press, Oxford, 1996.
- ICRP. Basic anatomical and physiological data for use in radiological protection: reference values. ICRP Publication 89. *Annals of the ICRP* 32. International Commission on Radiological Protection, Pergamon Press, Oxford, 2002.
- ICRP. The 2007 Recommendations of the International Commission on Radiological Protection. ICRP Publication 103. *Annals of the ICRP* 37(2-4). International Commission on Radiological Protection, Elsevier Ltd., 2007.

- ICRP. Nuclear decay data for dosimetric calculations. ICRP Publication 107. Annals of the ICRP 38. International Commission on Radiological Protection, Elsevier Ltd., 2008.
- ICRP. Conversion coefficients for radiological protection quantities for external radiation exposures. ICRP Publication 116. Annals of the ICRP 40. International Commission on Radiological Protection, Elsevier Ltd., 2010.
- ICRP. Dose coefficients for external exposures to environmental sources. ICRP Publication 144. Annals of the ICRP 49(2). International Commission on Radiological Protection, Elsevier Ltd., 2020.
- Ishikawa, T., S. Yasumura, K. Ozasa et al. The Fukushima Health Management Survey: estimation of external doses to residents in Fukushima Prefecture. *Sci Rep* 5: 12712 (2015).
- Jacob, P., H.G. Paretzke, H. Rosenbaum et al. Effective dose equivalents for photon exposures from plane sources on the ground. *Radiat Prot Dosim* 14(4): 299-310 (1986).
- Jacob, P. and R. Meckbach. Shielding factors and external dose evaluation. *Radiat Prot Dosim* 21(1-3): 79-85 (1987).
- Jacob, P. Exposures from external radiation and from inhalation of resuspended material. The First International Conference "The Radiological Consequences of the Chernobyl Accident" (A. Karaoglou et al., eds.). Minsk, Belarus, 1996.
- Jacob, P. and H.G. Paretzke. Gamma-ray exposure from contaminated soil. *Nucl Sci Eng* 93(3): 248-261 (2017).
- Kinase, S., T. Takahashi and K. Saito. Long-term predictions of ambient dose equivalent rates after the Fukushima Daiichi nuclear power plant accident. *J Nucl Sci Technol* 54(12): 1345-1354 (2017).
- Likhtarev, I.A., L.N. Kovgan, P. Jacob et al. Chernobyl accident: retrospective and prospective estimates of external dose of the population of Ukraine. *Health Phys* 82(3): 290-303 (2002).
- Matsuda, N., S. Mikami, T. Sato et al. Measurements of air dose rates in and around houses in the Fukushima Prefecture in Japan after the Fukushima accident. *J Environ Radioact* 166(Pt 3): 427-435 (2017).
- Meckbach, R. and P. Jacob. Gamma exposures due to radionuclides deposited in urban environments. Part II: Location factors for different deposition patterns. *Radiat Prot Dosim* 25(3): 181-190 (1988).
- MIC. Population census 2010. Ministry of Internal Affairs and Communications. [Internet] Available from (https://www.e-stat.go.jp/en/stat-search/files?page=1&toukei=00200521&bunya_1=02&tstat=000001039448&cycle=0&result_page=1&cycle_facet=cycle) on 23 March 2020.
- MIC. Housing and land survey: 2013 survey. Ministry of Internal Affairs and Communications. [Internet] Available from (<https://www.stat.go.jp/english/data/jyutaku/2501.html>) on 8 February 2015.
- MIC. Survey on time use and leisure activities: 2016 survey. Ministry of International Affairs and Communications. [Internet] Available from (<http://www.stat.go.jp/english/data/shakai/index.html>) 6 October 2017.
- Mikami, S., H. Tanaka, H. Matsuda et al. The deposition densities of radiocesium and the air dose rates in undisturbed fields around the Fukushima Dai-ichi nuclear power plant; their temporal changes for five years after the accident. *J Environ Radioact* 210: 105941 (2019).

- Miller, K.M., J.L. Kuiper and I.K. Helfer. ^{137}Cs fallout depth distributions in forest versus field sites: Implications for external gamma dose rates. *J Environ Radioact* 12(1): 23-47 (1990).
- Minamisoma City. Official communication from authorities of Minamisoma City and Naraha Town to the UNSCEAR secretariat. 2019.
- Minenko, V.F., A.V. Ulanovsky, V.V. Drozdovitch et al. Individual thyroid dose estimates for a case-control study of chernobyl-related thyroid cancer among children of Belarus--part II. Contributions from long-lived radionuclides and external radiation. *Health Phys* 90(4): 312-327 (2006).
- MOE. FY2014 Decontamination report - A compilation of experiences to date on decontamination for the living environment conducted by the Ministry of the Environment - March 2015. Ministry of the Environment, Japan. [Internet] Available from (http://josen.env.go.jp/en/policy_document/) on 10 September 2020a.
- MOE. Decontamination projects for radioactive contamination discharged by Tokyo Electric Power Company Fukushima Daiichi Nuclear Power Station accident, March 2018. Ministry of the Environment, Japan. [Internet] Available from (http://josen.env.go.jp/en/policy_document/) on 10 September 2020b.
- Murakami, M., S. Nomura, M. Tsubokura et al. Radiation doses and decontamination effects in Minamisoma city: airborne and individual monitoring after the Fukushima nuclear accident. *J Radiol Prot* 39(4): N27-N35 (2019).
- Muramatsu, Y., H. Matsuzaki, C. Toyama et al. Analysis of ^{129}I in the soils of Fukushima Prefecture: preliminary reconstruction of ^{131}I deposition related to the accident at Fukushima Daiichi Nuclear Power Plant (FDNPP). *J Environ Radioact* 139: 344-350 (2015).
- Nomura, S., M. Tsubokura, R. Hayano et al. Comparison between direct measurements and modeled estimates of external radiation exposure among school children 18 to 30 months after the Fukushima nuclear accident in Japan. *Environ Sci Technol* 49(2): 1009-1016 (2015).
- Nomura, S., M. Tsubokura, T. Furutani et al. Dependence of radiation dose on the behavioral patterns among school children: a retrospective analysis 18 to 20 months following the 2011 Fukushima nuclear incident in Japan. *J Radiat Res* 57(1): 1-8 (2016).
- Nomura, S., T. Oikawa and M. Tsubokura. Low dose from external radiation among returning residents to the former evacuation zone in Minamisoma City, Fukushima Prefecture. *J Radiol Prot* 39(2): 548-563 (2019).
- Nomura, S., M. Murakami, W. Naito et al. Low dose of external exposure among returnees to former evacuation areas: a cross-sectional all-municipality joint study following the 2011 Fukushima Daiichi nuclear power plant incident. *J Radiol Prot* 40(1): 1-18 (2020).
- Petoussi-Henss, N., H. Schlattl, M. Zankl et al. Organ doses from environmental exposures calculated using voxel phantoms of adults and children. *Phys Med Biol* 57(18): 5679-5713 (2012).
- Saito, K. and N. Petoussi-Henss. Ambient dose equivalent conversion coefficients for radionuclides exponentially distributed in the ground. *J Nucl Sci Technol* 51(10): 1274-1287 (2014).

- Saito, K., S. Mikami, M. Andoh et al. Temporal change in radiological environments on land after the Fukushima Daiichi Nuclear Power Plant accident. *J Radiat Prot Res* 44(4): 128-148 (2019a).
- Saito, K., S. Mikami, M. Andoh et al. Summary of temporal changes in air dose rates and radionuclide deposition densities in the 80 km zone over five years after the Fukushima Nuclear Power Plant accident. *J Environ Radioact* 210: 105878 (2019b).
- Satoh, D., T. Furuta, F. Takahashi et al. Simulation study of personal dose equivalent for external exposure to radioactive cesium distributed in soil. *J Nucl Sci Technol* 54(9): 1018-1027 (2017).
- Schimmack, W., H. Steindl and K. Bunzl. Variability of water content and of depth profiles of global fallout ^{137}Cs in grassland soils and the resulting external gamma-dose rates. *Radiat Environ Biophys* 37(1): 27-33 (1998).
- Takahara, S., T. Abe, M. Iijima et al. Statistical characterization of radiation doses from external exposures and relevant contributors in Fukushima prefecture. *Health Phys* 107(4): 326-335 (2014).
- Tsubokura, M., S. Kato, T. Morita et al. Assessment of the annual additional effective doses amongst Minamisoma children during the second year after the Fukushima Daiichi Nuclear Power Plant disaster. *PLoS One* 10(6): e0129114 (2015).
- Tsubokura, M., M. Murakami, S. Nomura et al. Individual external doses below the lowest reference level of 1 mSv per year five years after the 2011 Fukushima nuclear accident among all children in Soma City, Fukushima: A retrospective observational study. *PLoS One* 12(2): e0172305 (2017).
- Tsubokura, M., S. Nomura, I. Yoshida et al. Comparison of external doses between radio-contaminated areas and areas with high natural terrestrial background using the individual dosimeter 'D-shuttle' 75 months after the Fukushima Daiichi nuclear power plant accident. *J Radiol Prot* 38(1): 273-285 (2018).
- Tsubokura, M., M. Murakami, Y. Takebayashi et al. Impact of decontamination on individual radiation doses from external exposure among residents of Minamisoma City after the 2011 Fukushima Daiichi nuclear power plant incident in Japan: a retrospective observational study. *J Radiol Prot* 39(3): 854-871 (2019).
- Ulanovsky, A., P. Jacob, S. Fesenko et al. ReSCA: decision support tool for remediation planning after the Chernobyl accident. *Radiat Environ Biophys* 50(1): 67-83 (2011).
- UNSCEAR. Sources and Effects of Ionizing Radiation. Volume II: Effects. Scientific Annexes C, D and E. UNSCEAR 2008 Report. United Nations Scientific Committee on the Effects of Atomic Radiation. United Nations sales publication E.11.IX.3. United Nations, New York, 2011.
- UNSCEAR. Sources, Effects and Risks of Ionizing Radiation. Volume I: Report to the General Assembly and Scientific Annex A. UNSCEAR 2013 Report. United Nations Scientific Committee on the Effects of Atomic Radiation. United Nations sales publication E.14.IX.1. United Nations, New York, 2014.
- WHO. Preliminary dose estimation from the nuclear accident after the 2011 Great East Japan earthquake and tsunami. World Health Organization, Geneva, 2012.
- WHO. Health risk assessment from the nuclear accident after the 2011 Great East Japan earthquake and tsunami. World Health Organization, Geneva, Switzerland, 2013.